Magneto-optical properties of bilayer Bernal graphene

何彦宏[a,b]，邱裕煌[a]，林德鴻[b]，林明發[a]

[a]國立成功大學 物理系
[b]國立中山大學 物理系

- **Electronic structures**
  … *Peierls tight-binding model*
- **Optical excitations**
  … *Gradient approximation*
- **Result discussion**
- **Summary**

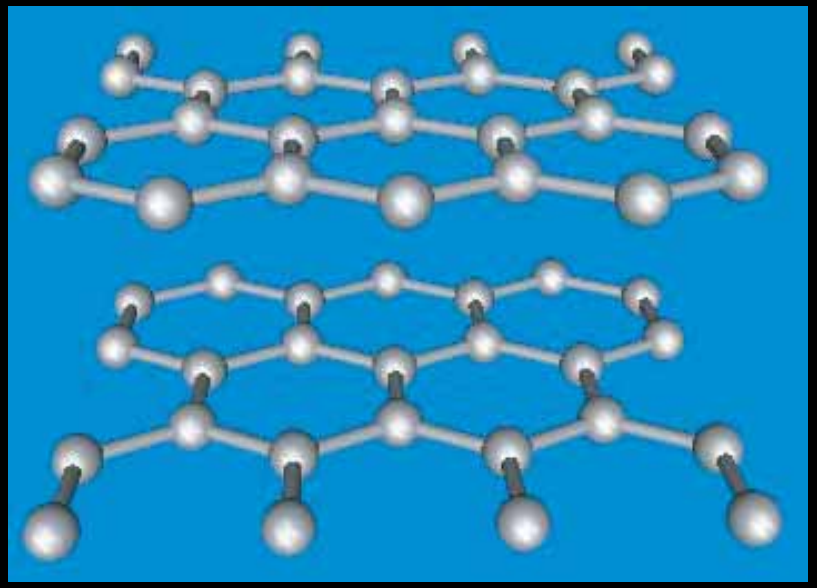

Motive: Graphene related systems

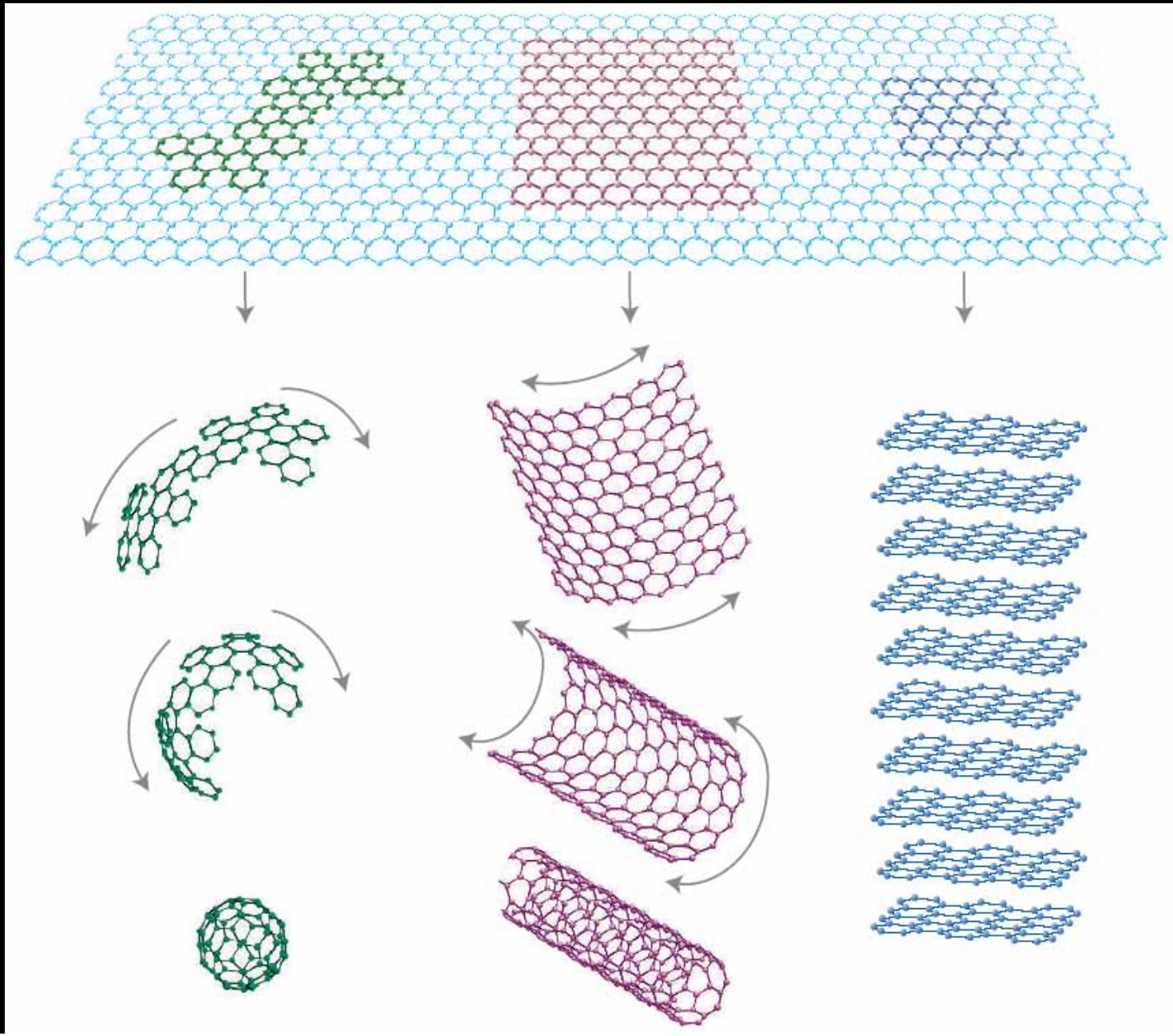

Motive: Few-layered graphene

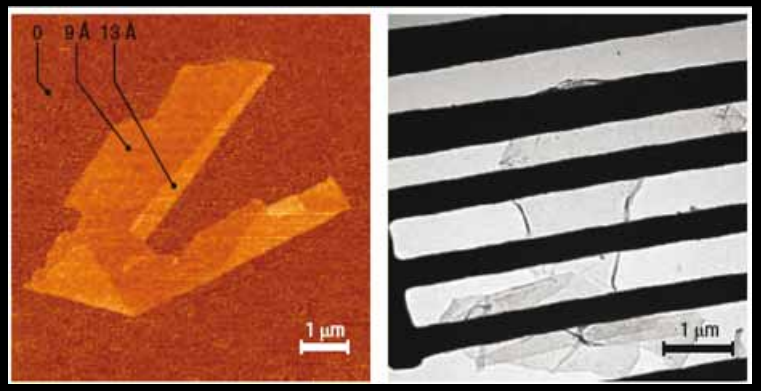

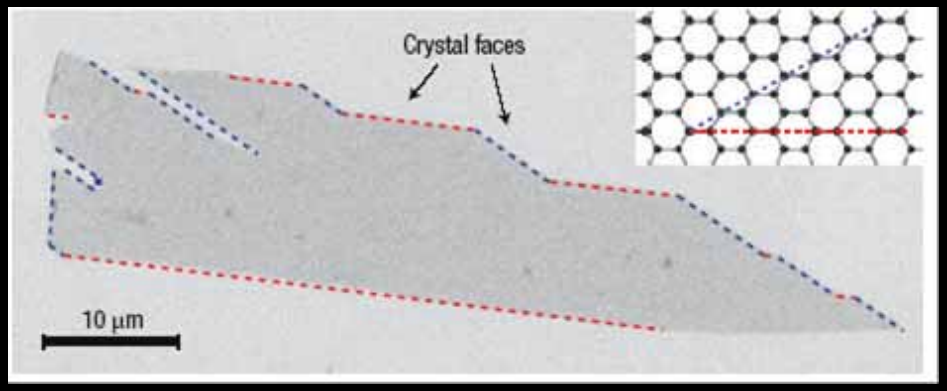

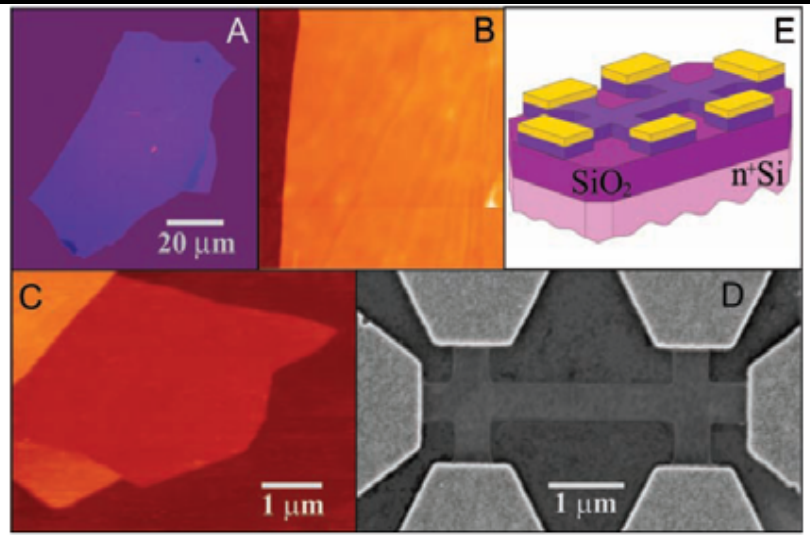

Fig. 1. Graphene films. (**A**) Photograph (in normal white light) of a relatively large multilayer graphene flake with thickness ~3 nm on top of an oxidized Si wafer. (**B**) Atomic force microscope (AFM) image of 2 μm by 2 μm area of this flake near its edge. Colors: dark brown, SiO_2 surface; orange, 3 nm height above the SiO_2 surface. (**C**) AFM image of single-layer graphene. Colors: dark brown, SiO_2 surface; brown-red (central area), 0.8 nm height; yellow-brown (bottom left), 1.2 nm; orange (top left), 2.5 nm. Notice the folded part of the film near the bottom, which exhibits a differential height of ~0.4 nm. For details of AFM imaging of single-layer graphene, see (*15*). (**D**) Scanning electron microscope image of one of our experimental devices prepared from FLG. (**E**) Schematic view of the device in (D).

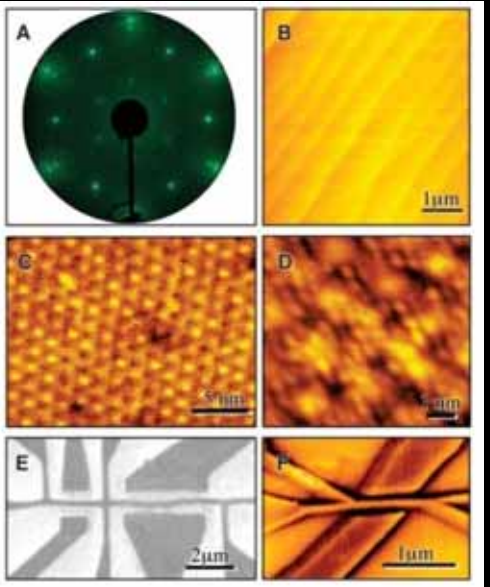

Fig. 1. Production and characterization of EG. (**A**) LEED pattern (71 eV) of three monolayers of EG on 4H-SiC(000$\bar{1}$) (C-terminated face). The outermost hexagon (spots aligned on the vertical) is graphene 1×1 diffraction. Bright sixfold spots aligned on the horizontal are SiC 1×1. The smallest hexagon is the result of a $\sqrt{3} \times \sqrt{3}$ reconstruction of the interfacial layer, as are the spots lying just inside the graphene pattern. Graphene thickness is determined via Auger spectroscopy (attenuation of Si peaks). (**B**) AFM image of graphitized 4H-SiC, showing extended terraces. STM studies indicate that the graphite is continuous over the steps (*J*). (**C**) STM image of one monolayer of EG on SiC(0001). Tunneling conditions (tip bias −0.8 V, current 100 pA) preferentially image structure beneath the graphene layer. Two interface corrugations are apparent, with periods 6×6 (1.8-nm triangular superlattice) and $\sqrt{3} \times \sqrt{3}$ (smaller spots with 0.54-nm spacing) relative to the SiC surface unit cell. (**D**) STM image of interface reconstruction beneath one monolayer of graphene on SiC(0001) obtained after lithography. General features are as seen in (C). (**E**) SEM of patterned EG. Dark regions are the EG (still coated with electron-beam resist). (**F**) EFM of another patterned EG sample, showing a horizontal ribbon (bright contrast) with tapered voltage contacts left and right, which is flanked by diagonally oriented side gates above and below the ribbon. Contrast is obtained through electrostatic forces between the probe and the graphene structure to which potentials are applied, thus allowing functioning devices to be measured.

Mechanical exfoliation of highly oriented pyrolytic graphite ***Science* 306**, 666 (2004)

Epitaxial growth on silicon carbide ***Science* 312**, 1191 (2006)

Low-energy states at B_0=0: monolayer & bilayer Bernal graphene

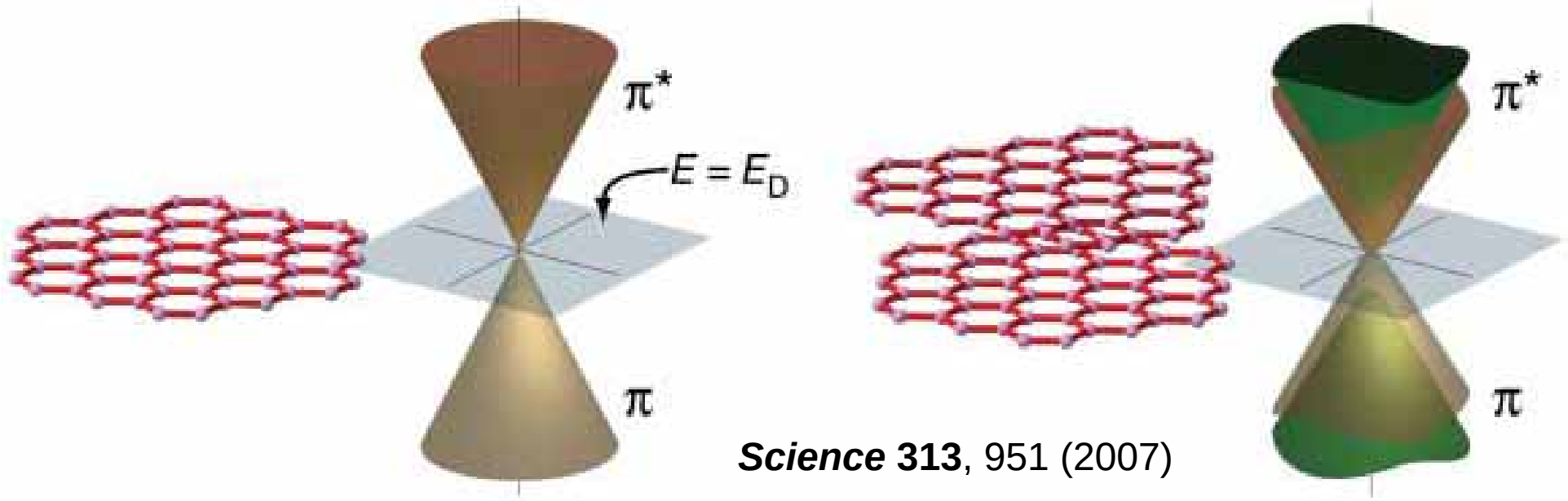

***Science* 313**, 951 (2007)

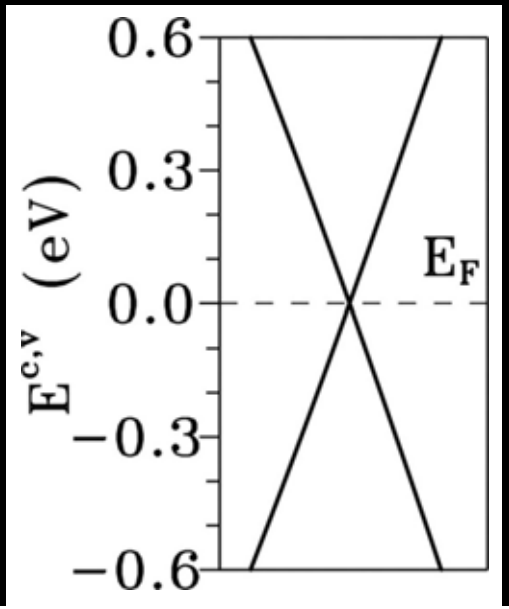

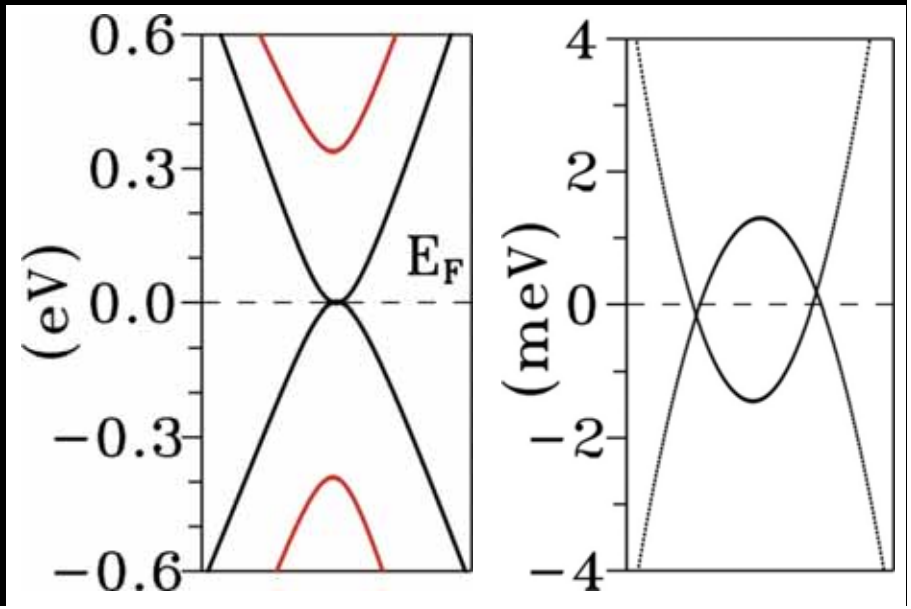

Landau level quantization

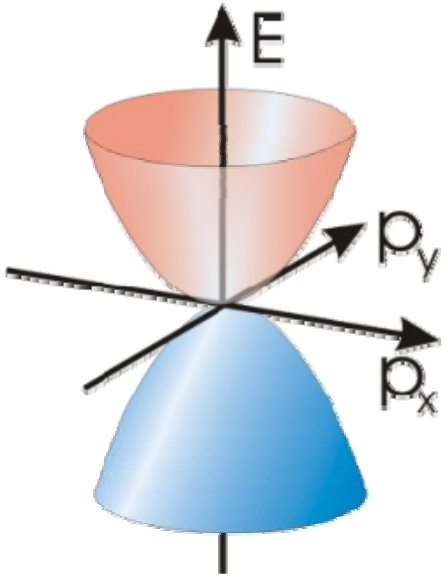

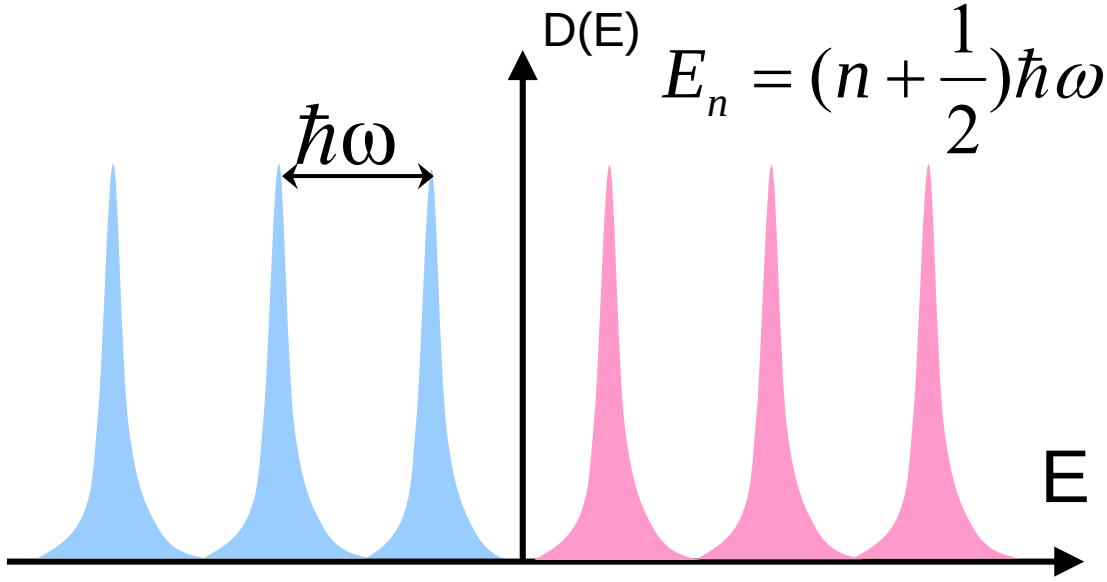

$$E_n = (n + \frac{1}{2})\hbar\omega$$

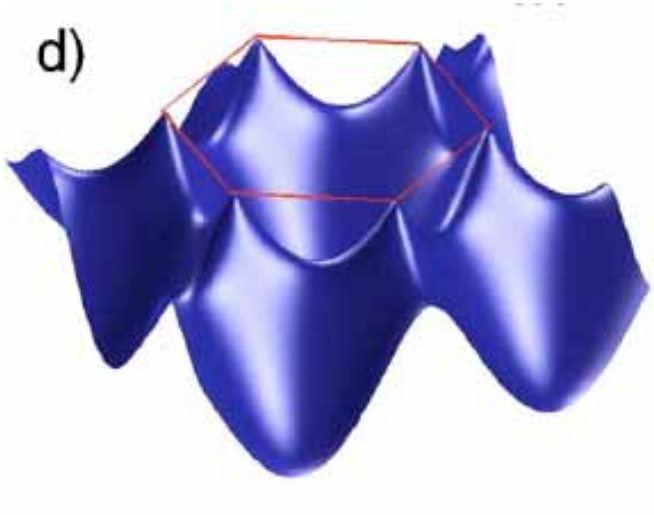

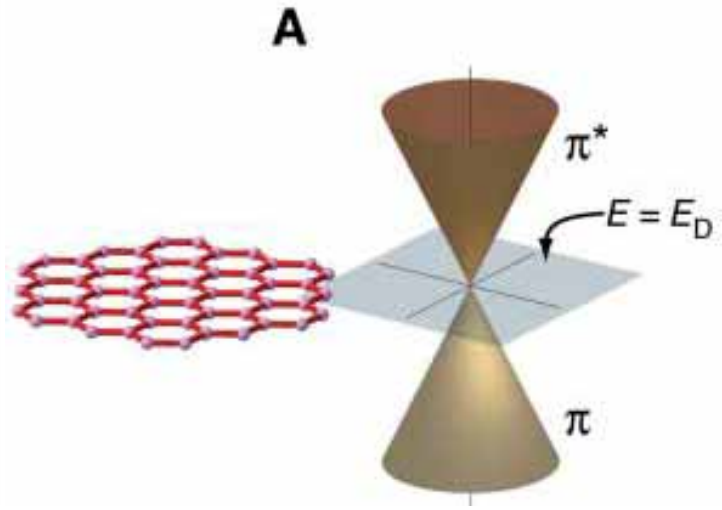

$$E_n^{c,v} \propto \sqrt{n^{c,v} B_0}$$

Experimental observation of Landau levels in graphene

Quantum Hall conductivity;
Scanning tunneling spectroscopy
Magnetooptical transmission
(excitations between Landau levels)

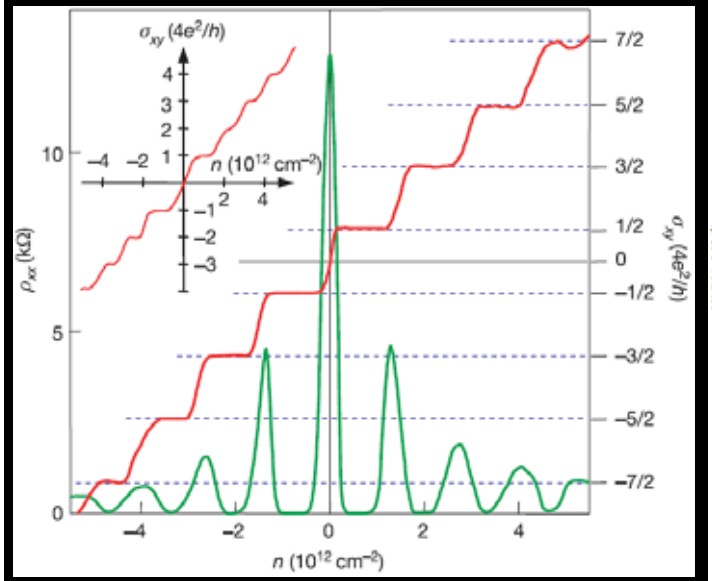

***Nature* 438**, 197 (2005)

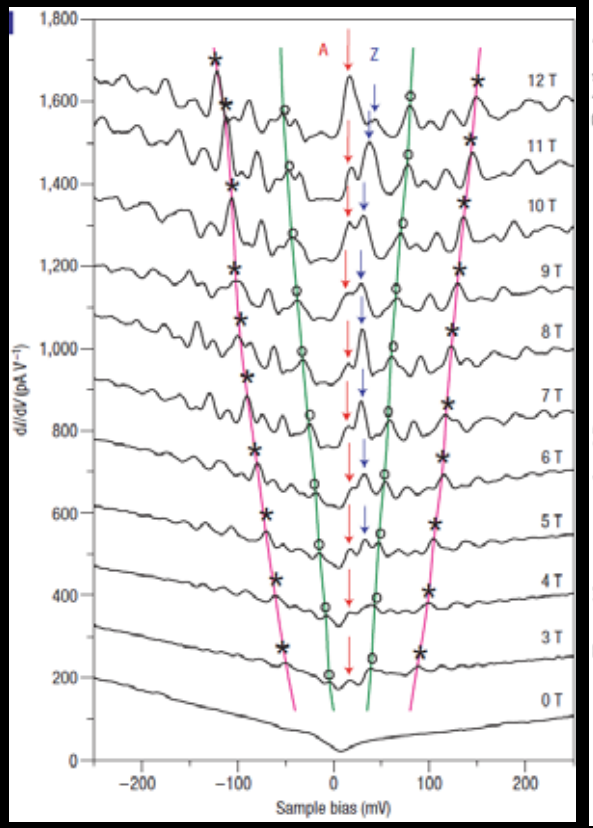

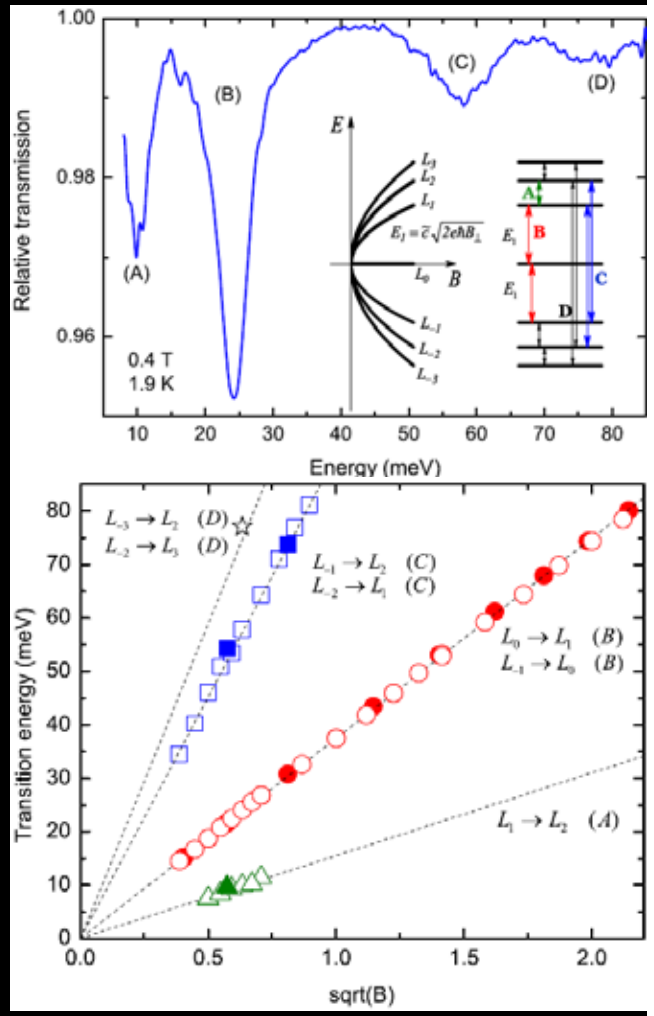

***Nat. Phys.* 3**, 623 (2007) ***PRL* 97**, 266405 (2006)

Tight-binding model ***Phys. Rev.* 109,** 272 (1958)

$$\psi_k(\vec{r}) = u_k(\vec{r}) \exp(i\vec{k} \cdot \vec{r})$$

monolayer graphene

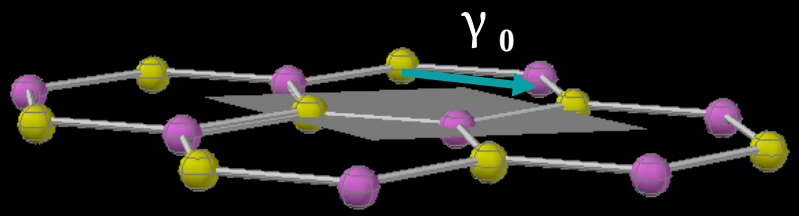

$$|\Phi\rangle = \quad A|A\rangle + B|B\rangle$$

$$\langle A|H|B\rangle \longrightarrow \gamma_0 \ (2.598 \text{ eV})$$

bilayer Bernal graphene

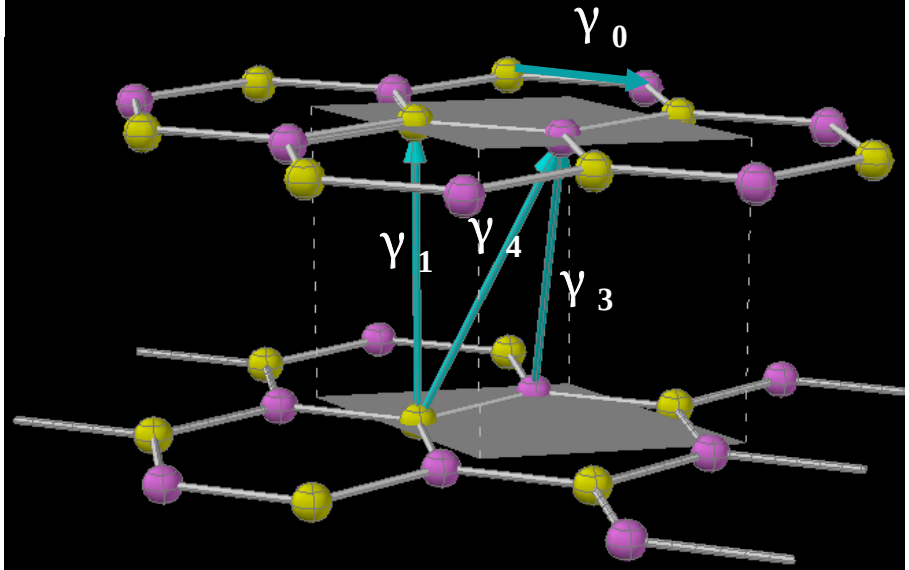

$$|\Phi\rangle = \quad A_1|A_1\rangle + B_1|B_1\rangle + A_2|A_2\rangle + B_2|B_2\rangle$$

$$\langle A_1|H|B_1\rangle \longrightarrow \gamma_0 \ (2.598 \text{ eV})$$

$$\langle A_1|H|A_2\rangle \longrightarrow \gamma_1 \ (0.364 \text{ eV})$$

$$\langle B_1|H|B_2\rangle \longrightarrow \gamma_3 \ (0.319 \text{ eV})$$

$$\langle A_1|H|B_2\rangle \longrightarrow \gamma_4 \ (0.177 \text{ eV})$$

$$\langle A_2|H|A_2\rangle \longrightarrow \gamma_6 \ (-0.026 \text{ eV})$$

Peierls tight-binding model

$$\Phi(\vec{k},\vec{r}) = \frac{1}{\sqrt{N}}\sum_{\vec{R}} e^{i\vec{k}\cdot\vec{r}}\phi(\vec{r}-\vec{R})\cdot\exp(i\frac{e}{\hbar}\int_{\vec{R}}^{\vec{r}}\vec{A}\cdot d\vec{r})$$

$$H = \frac{1}{2m}(\vec{p}-e\vec{A})^2 + V(\vec{r}),$$

$$H\Phi(\vec{k},\vec{r}) = \frac{1}{\sqrt{N}}\sum_{\vec{R}} e^{i\vec{k}\cdot\vec{R}}\cdot\exp(i\frac{e}{\hbar}\int_{\vec{R}}^{\vec{r}}\vec{A}\cdot d\vec{r})[\frac{\vec{p}^2}{2m}+V(\vec{r})]\phi(\vec{r}-\vec{R})$$

$$\langle\Phi(\vec{k'},\vec{r'})|H|\Phi(\vec{k},\vec{r})\rangle = \frac{1}{\sqrt{N}}\sum_{\vec{R'},\vec{R}} e^{i(\vec{k}\cdot\vec{R}-\vec{k'}\cdot\vec{R'})}\langle\phi(\vec{r'}-\vec{R'})|\frac{\vec{p}^2}{2m}+V(\vec{r})|\phi(\vec{r}-\vec{R})\rangle\cdot\exp(i\frac{e}{\hbar}\int_{\vec{R}}^{\vec{R'}}\vec{A}\cdot d\vec{r})$$

***Phys. Rev.* 84,** 814 (1951)

For $\vec{A}=(0,Bx,0)$ $(\vec{B}=\nabla\times\vec{A}=B\hat{z})$

$$\langle\Phi(\vec{k'},\vec{r'})|H|\Phi(\vec{k},\vec{r})\rangle = \frac{1}{\sqrt{N}}\sum_{\vec{R'},\vec{R}} e^{i(\vec{k}\cdot\vec{R}-\vec{k'}\cdot\vec{R'})}\langle\phi(\vec{r'}-\vec{R'})|\frac{\vec{p}^2}{2m}+V(\vec{r})|\phi(\vec{r}-\vec{R})\rangle\cdot\exp\{\pm i\pi\frac{\phi}{\phi_0}[(j-1)+\frac{1}{6}]\}$$

$\frac{\phi}{\phi_0}=\frac{1}{R_B}$; ϕ_0=h/e=4.1356×10^{15} T/m^2; ϕ_0 ~79000 T through a hexagon

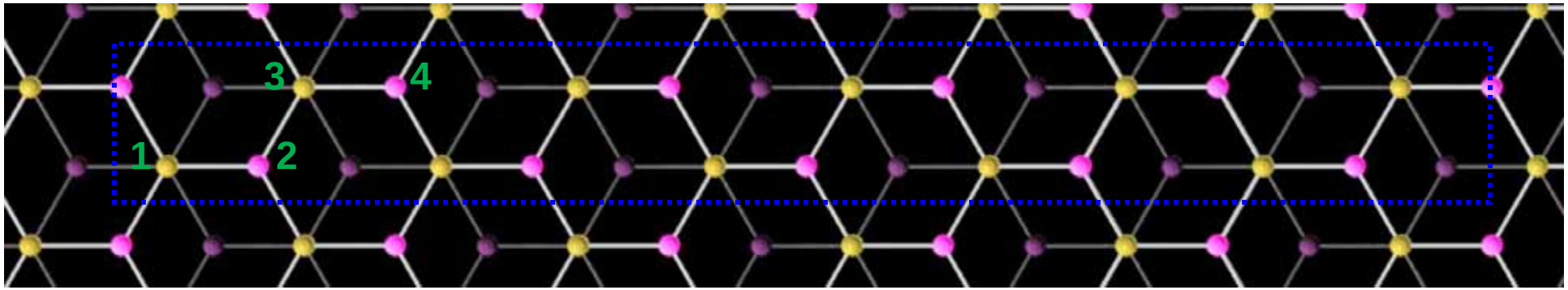

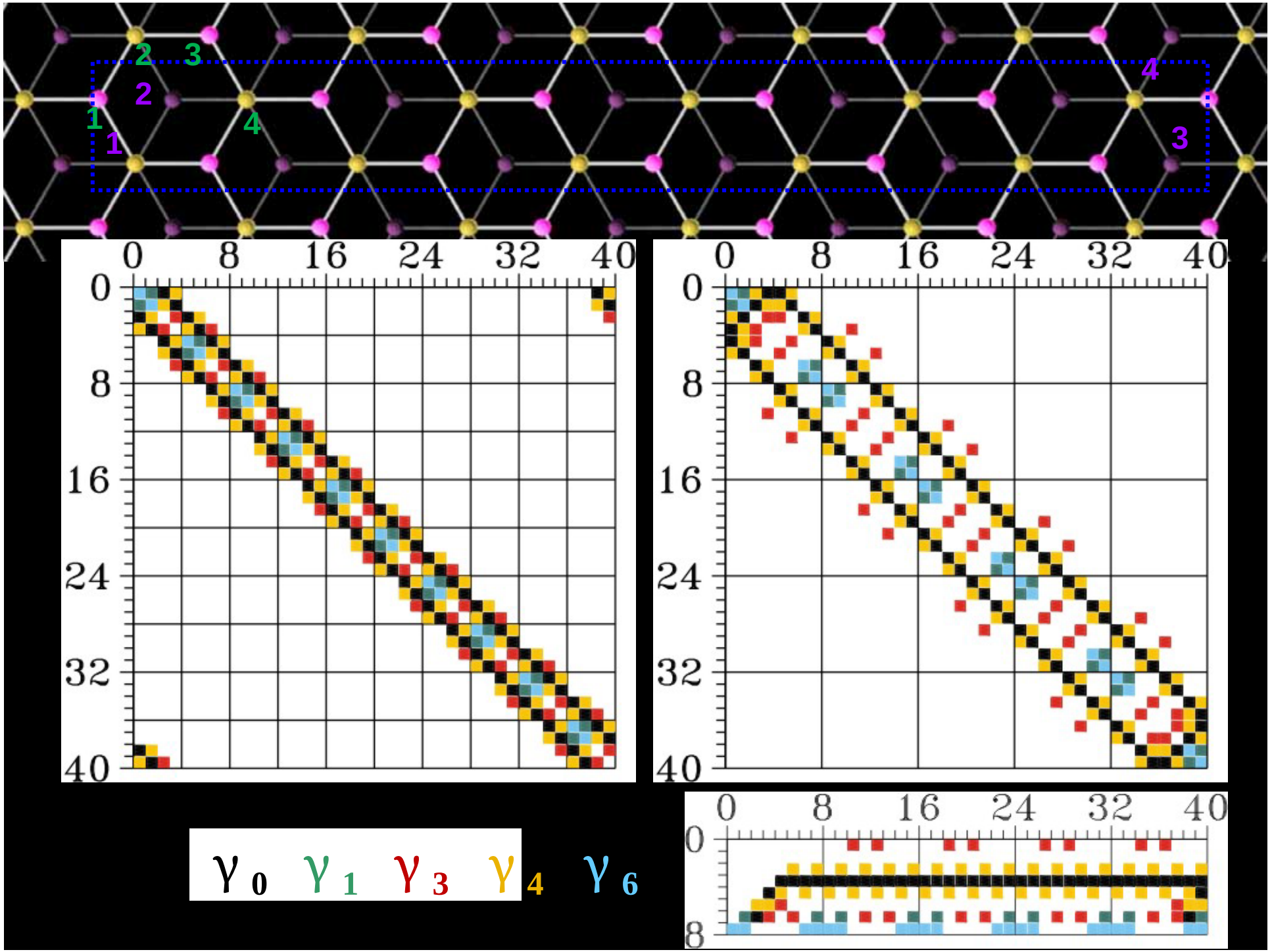
2
3
2
1
1
4
4
3
0
8
16
24
32
40
γ_0 γ_1 γ_3 γ_4 γ_6

Monolayer: Landau-level energies

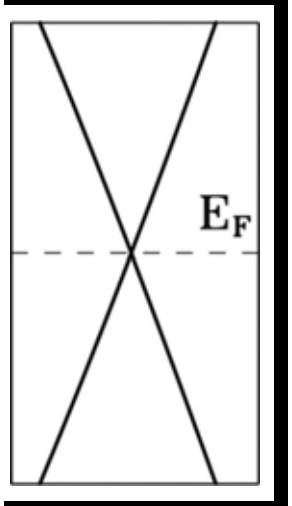

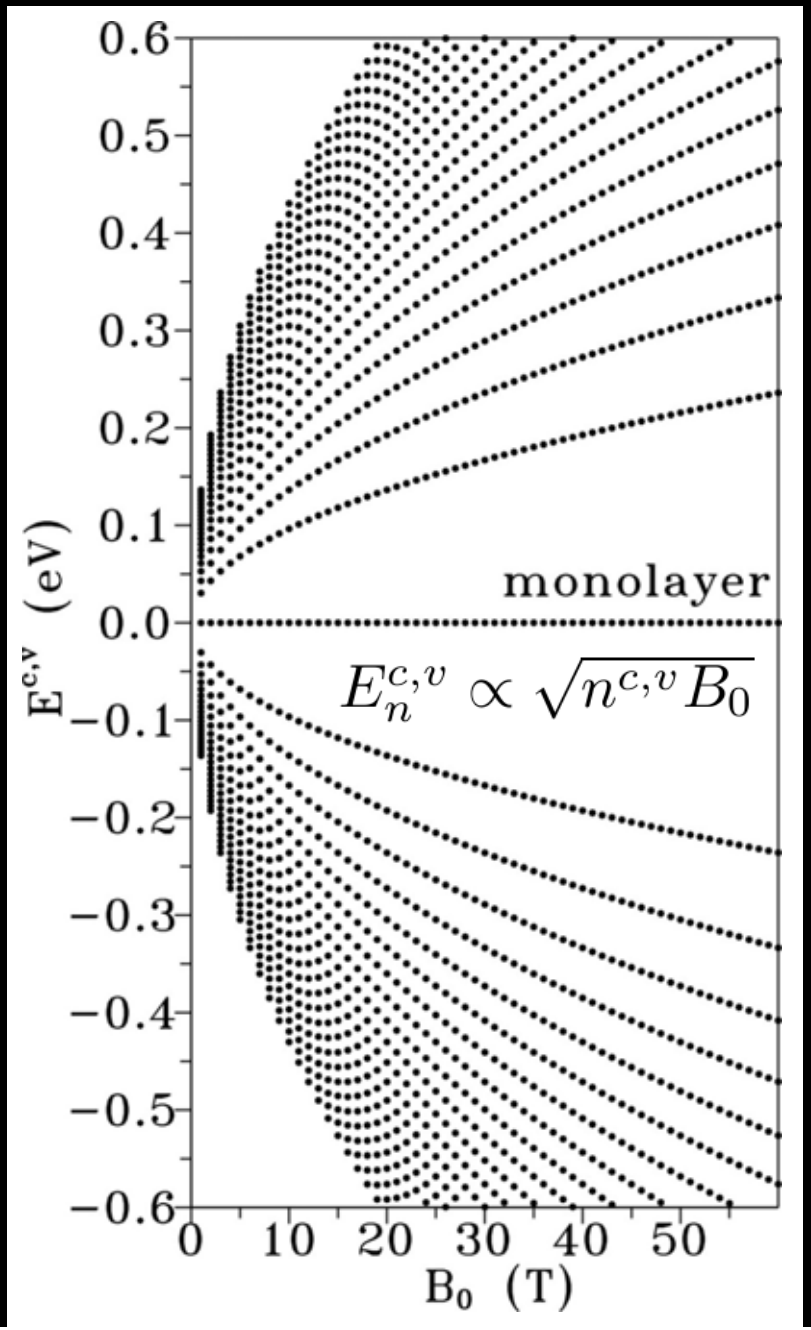

Monolayer: Landau-level energies & density of states

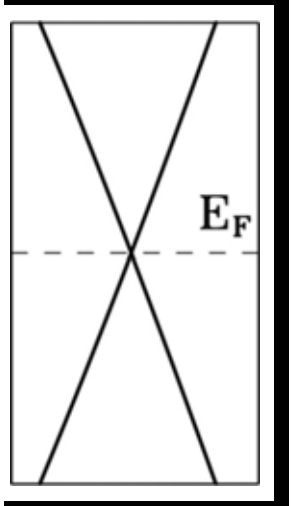

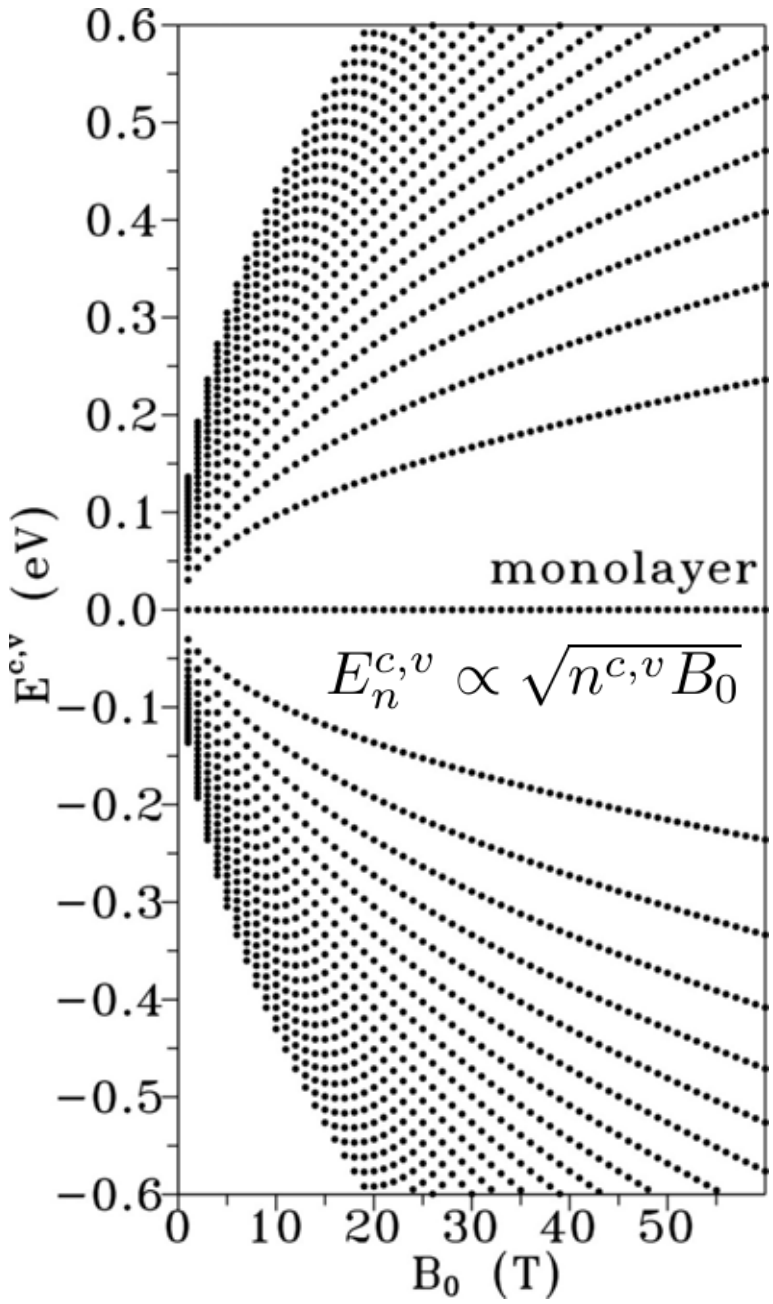

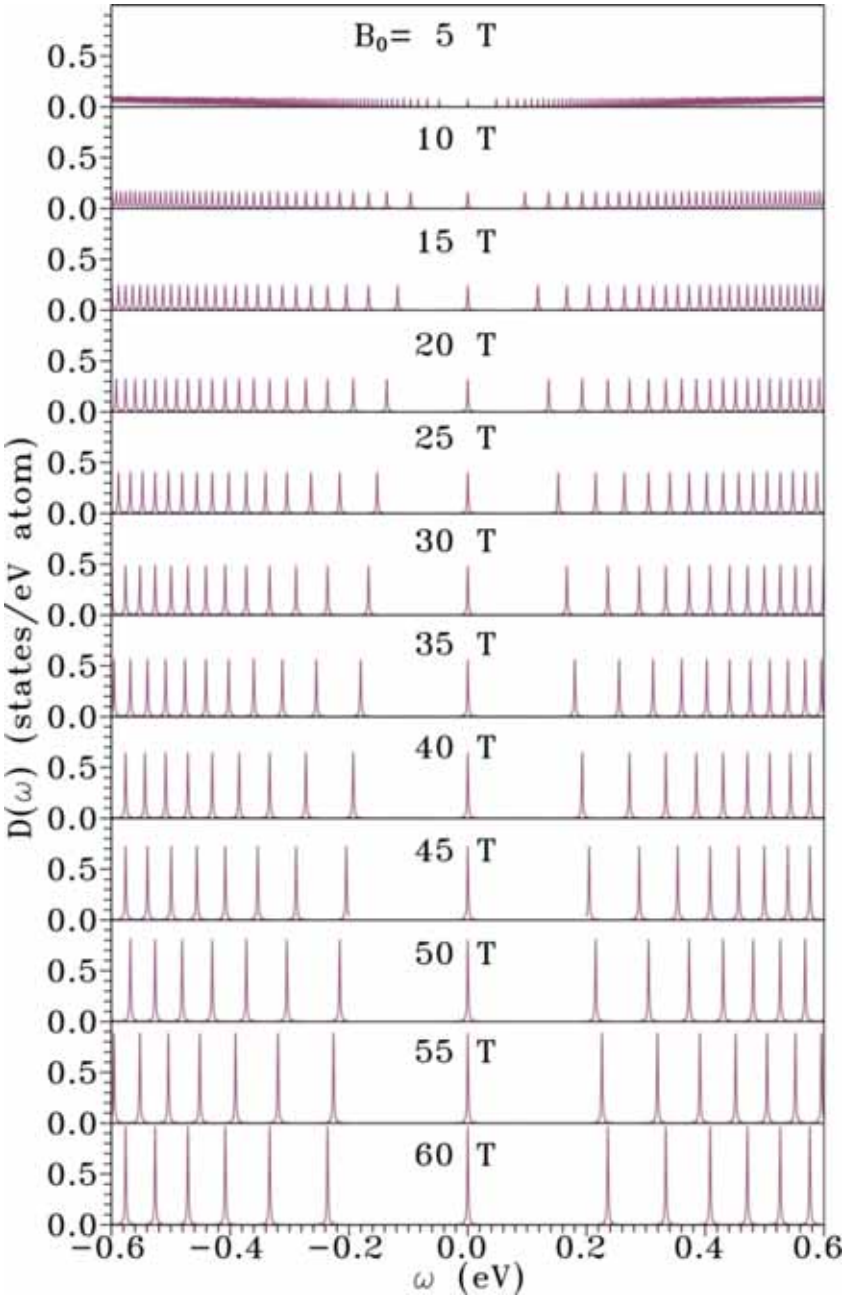

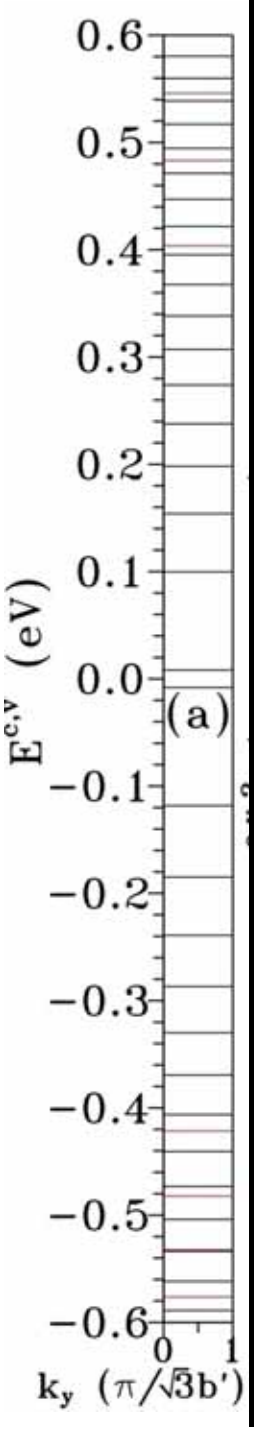

Bilayer Bernal graphene: Landau level at 40 T

Subband asymmetry

Each fourfold degenerate

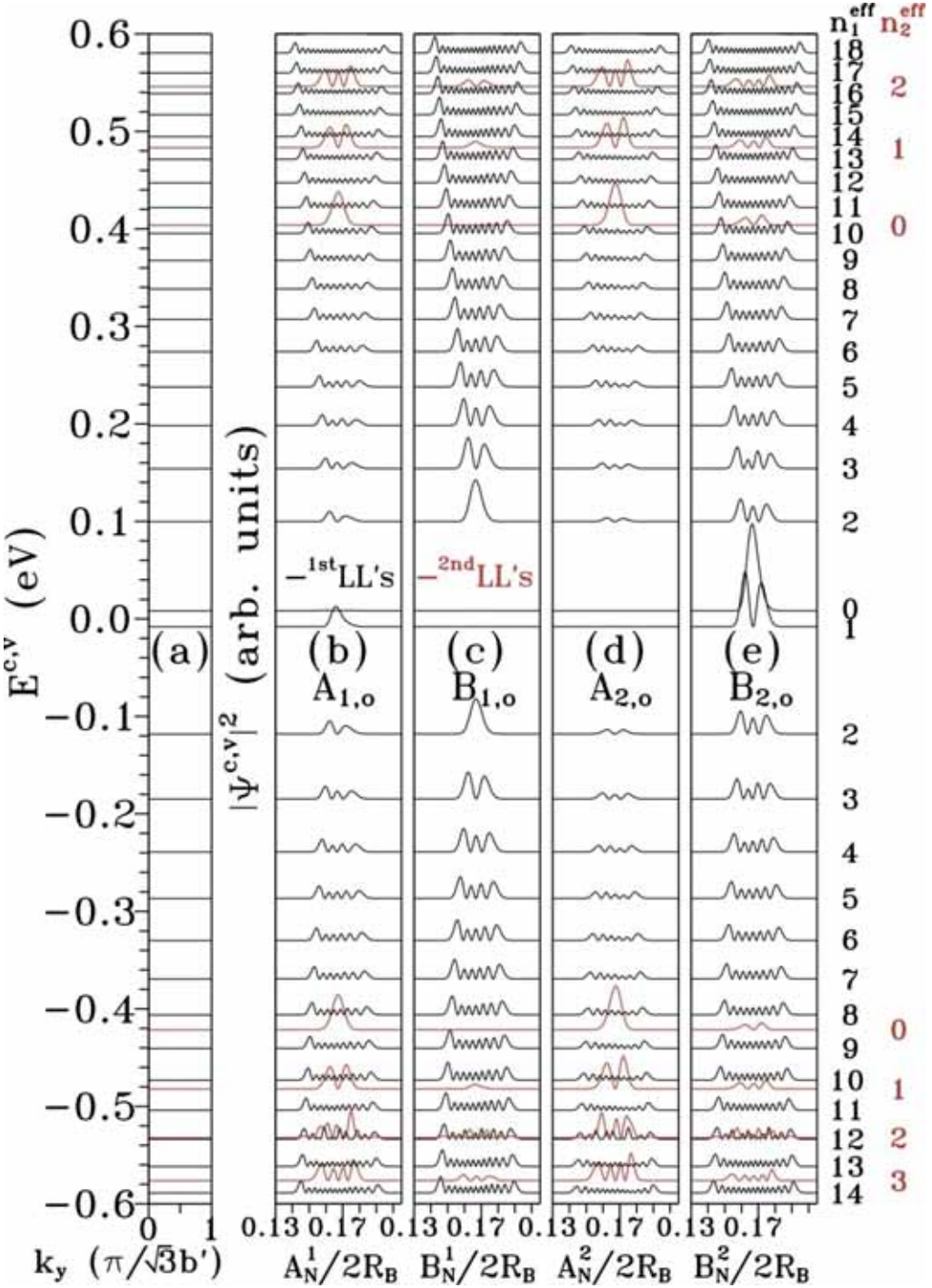

Bilayer Bernal graphene: energy and wave function of Landau level at 40 T

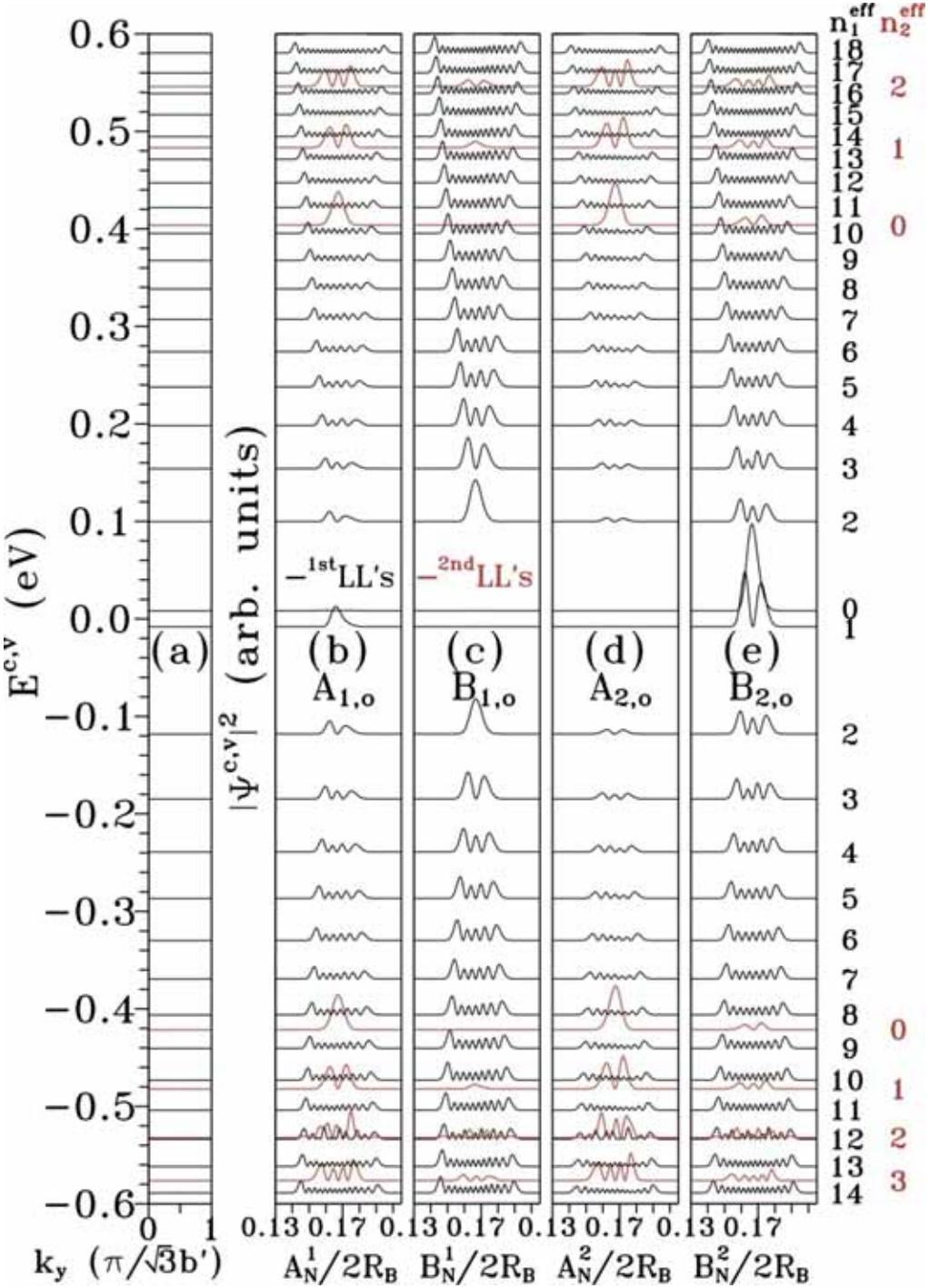

Bilayer Bernal graphene: energy and wave function of Landau level at 40 T

1st group-Landau levels (by B atoms)

2nd group-Landau levels (by A atoms)

Bilayer: Landau-level energies

0.34 eV $(\gamma_1+\gamma_6)$

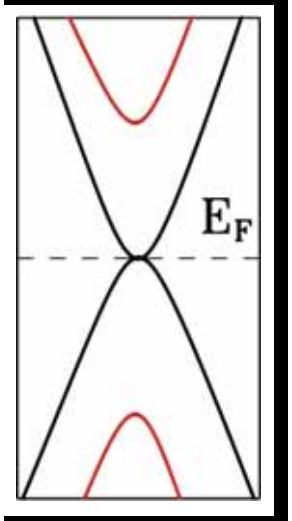

-0.39 eV $(-\gamma_1+\gamma_6)$

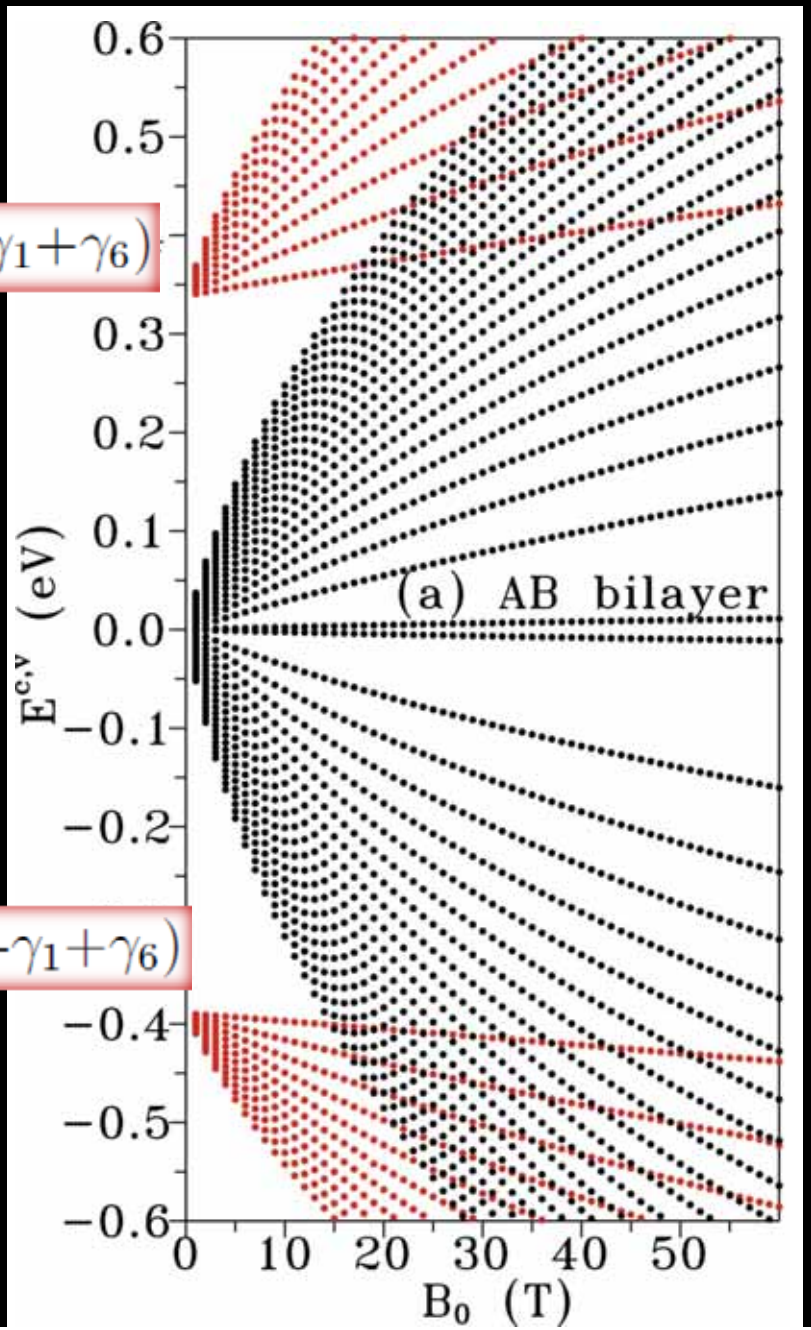

Bilayer: Landau-level energies & density of states

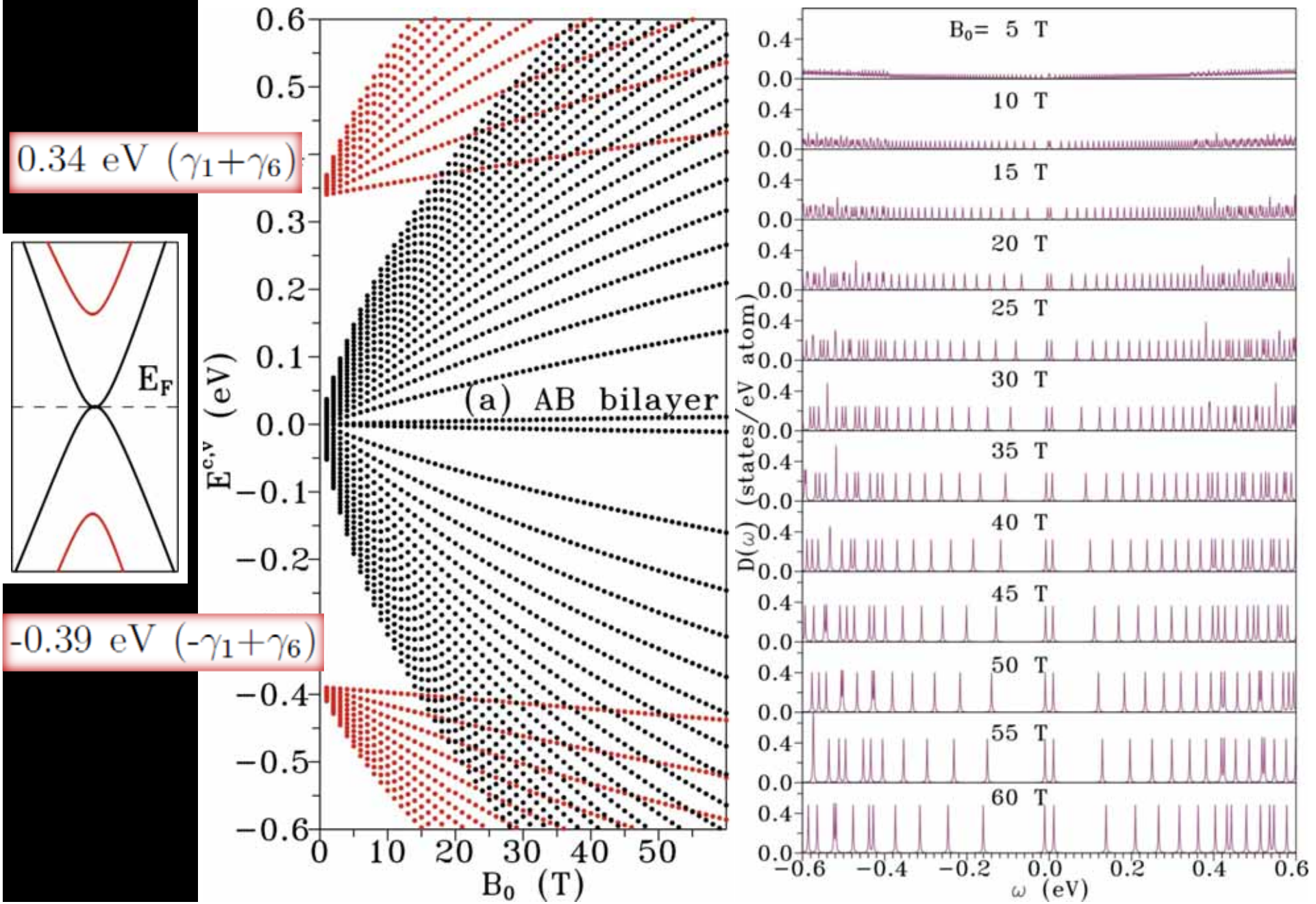

Optical absorption spectra: *gradient approximation*

absorption rate: $W(\vec{q} \sim 0, \omega) = \sum_{i,j} P_{i\to j} - P_{j\to i}$

$$= \frac{2\pi}{\hbar}(\frac{eA_0}{mc})^2 2 \sum_{i,j} |\langle \Phi_j | e^{i\vec{q}\cdot\vec{r}} \hat{e}\cdot\vec{p} | \Phi_i \rangle|^2 \delta(E_j - E_i + \hbar\omega)[f(E_i) - f(E_j)]$$

dipole matrix element within the gradient approximation

$$\langle \Phi_j | \vec{p} | \Phi_i \rangle = \langle \Phi_j | \frac{im}{\hbar}[H, \vec{r}] | \Phi_i \rangle$$

$$= \frac{im}{\hbar}(\vec{R}_i - \vec{R}_j)\langle \Phi_j | H | \Phi_i \rangle$$

$$= \frac{m}{\hbar} \nabla_{\vec{k}} \langle \Phi_j | H | \Phi_j \rangle$$

Fermi-Dirac distribution function:

$$f(E_{i,j}) = \frac{1}{\exp\{[E_{i,j} - \mu(T)]/k_B T\} + 1}$$

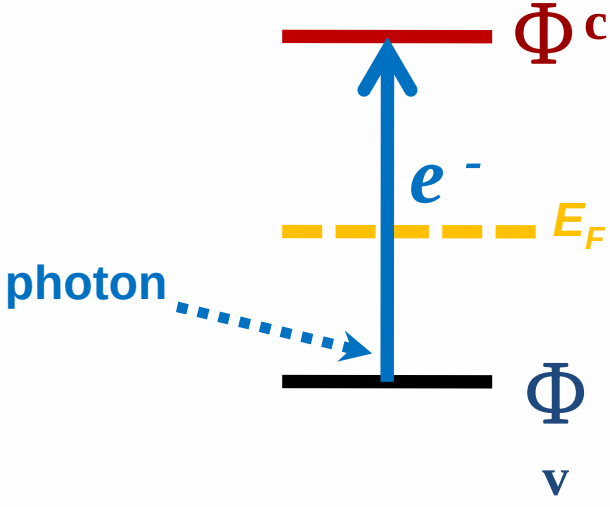

Optical absorption spectra

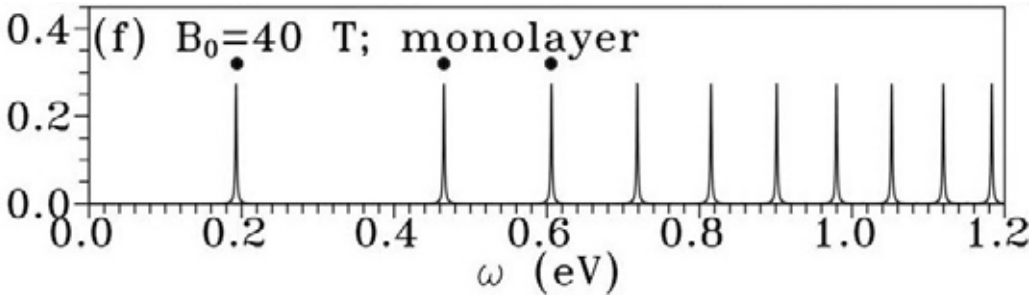

Optical absorption spectra

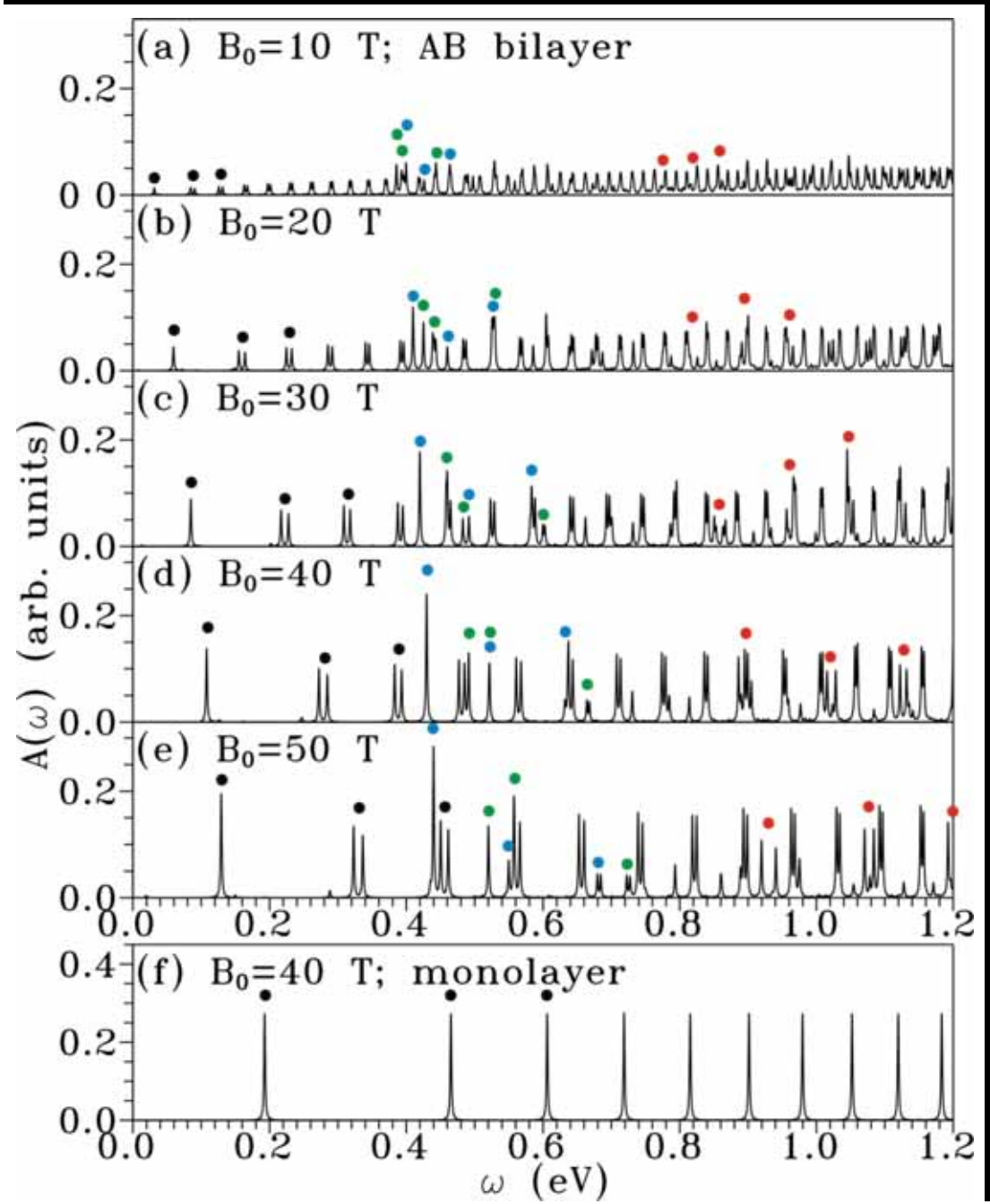

Optical absorption spectra

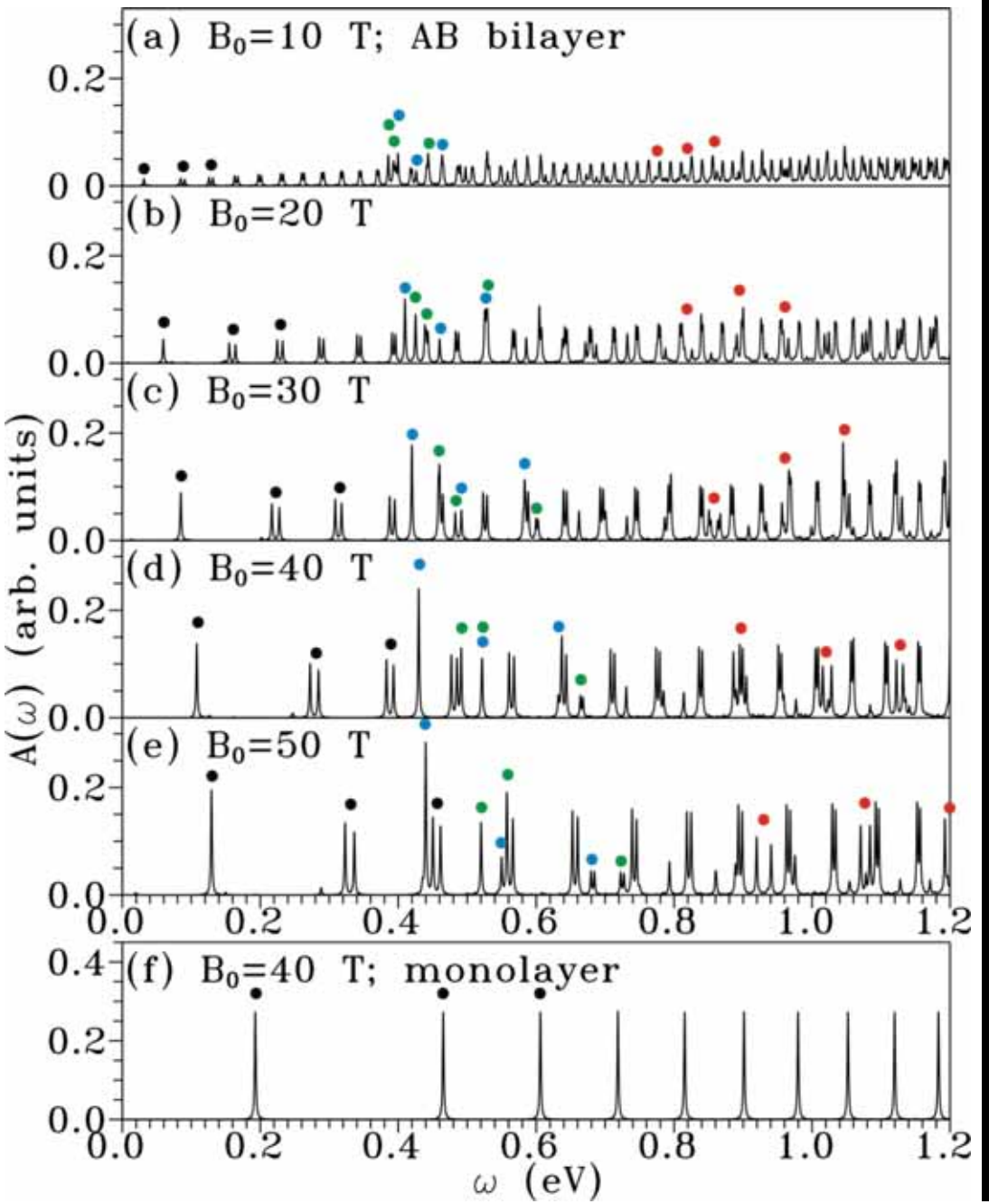

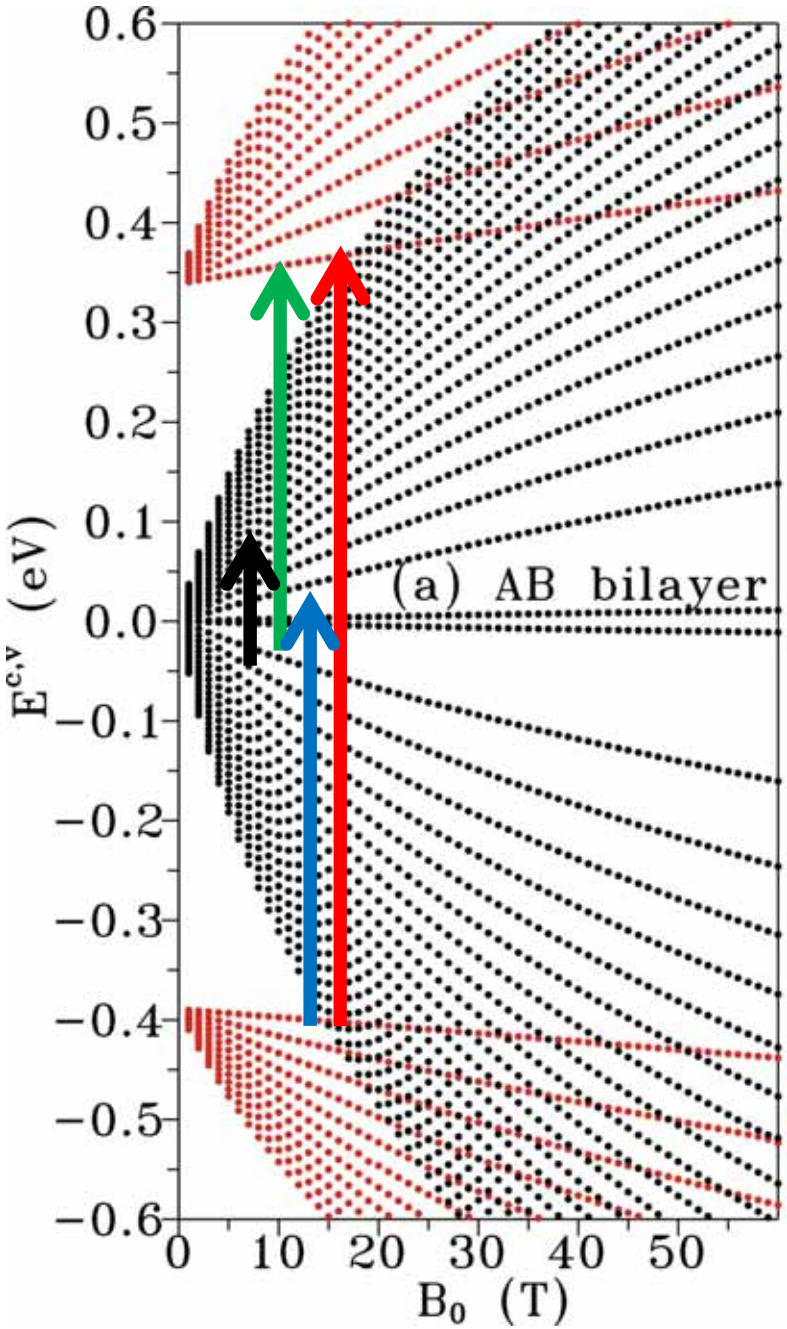

Optical absorption spectra

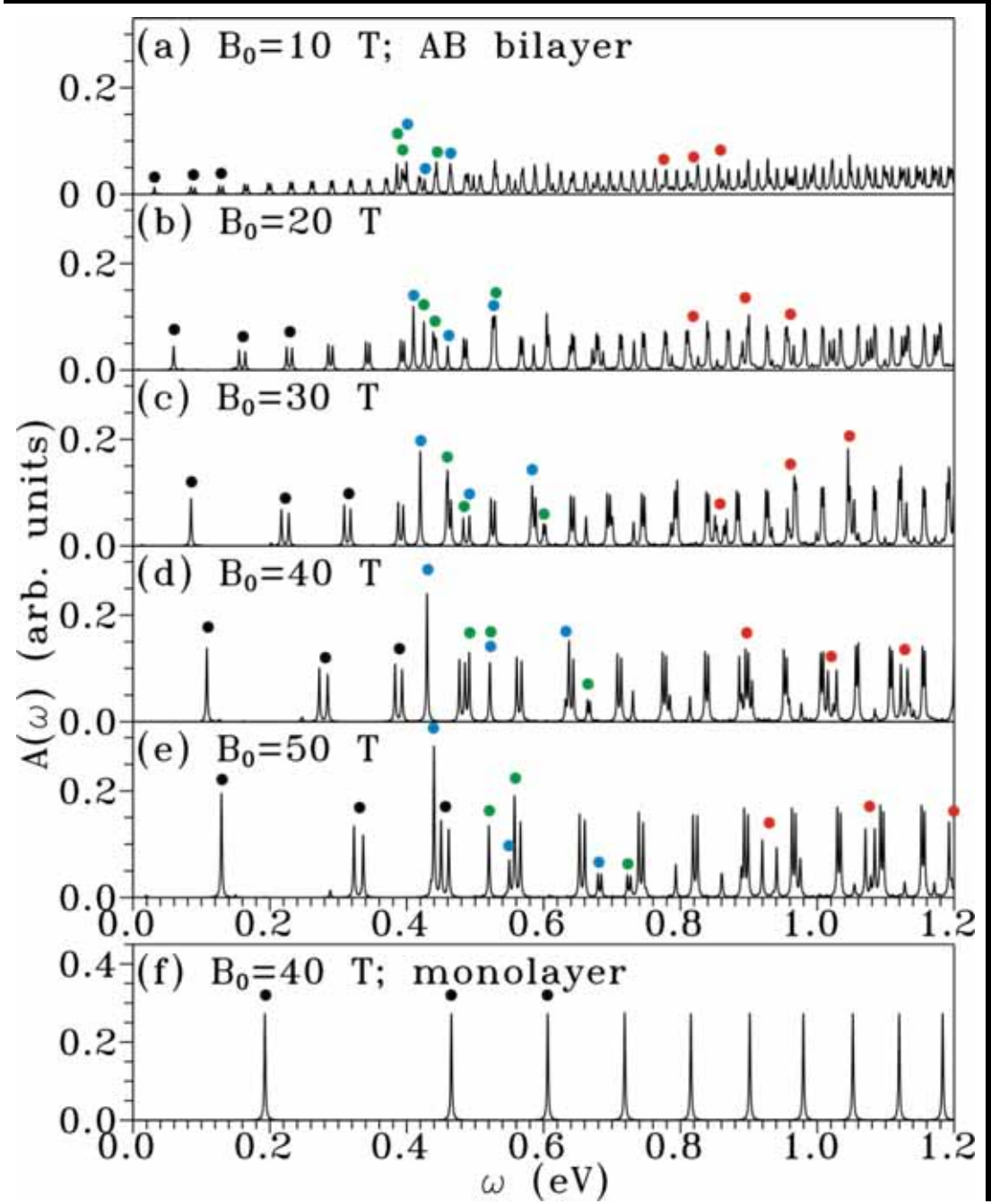

Selection rules

$$n_1^c - n_1^v = 1, -1$$

$$n_2^c - n_2^v = 1, -1$$

$$n_1^v - n_2^c = 0, 2$$

$$n_1^c - n_2^v = 0, 2$$

B-dependent absorption frequencies

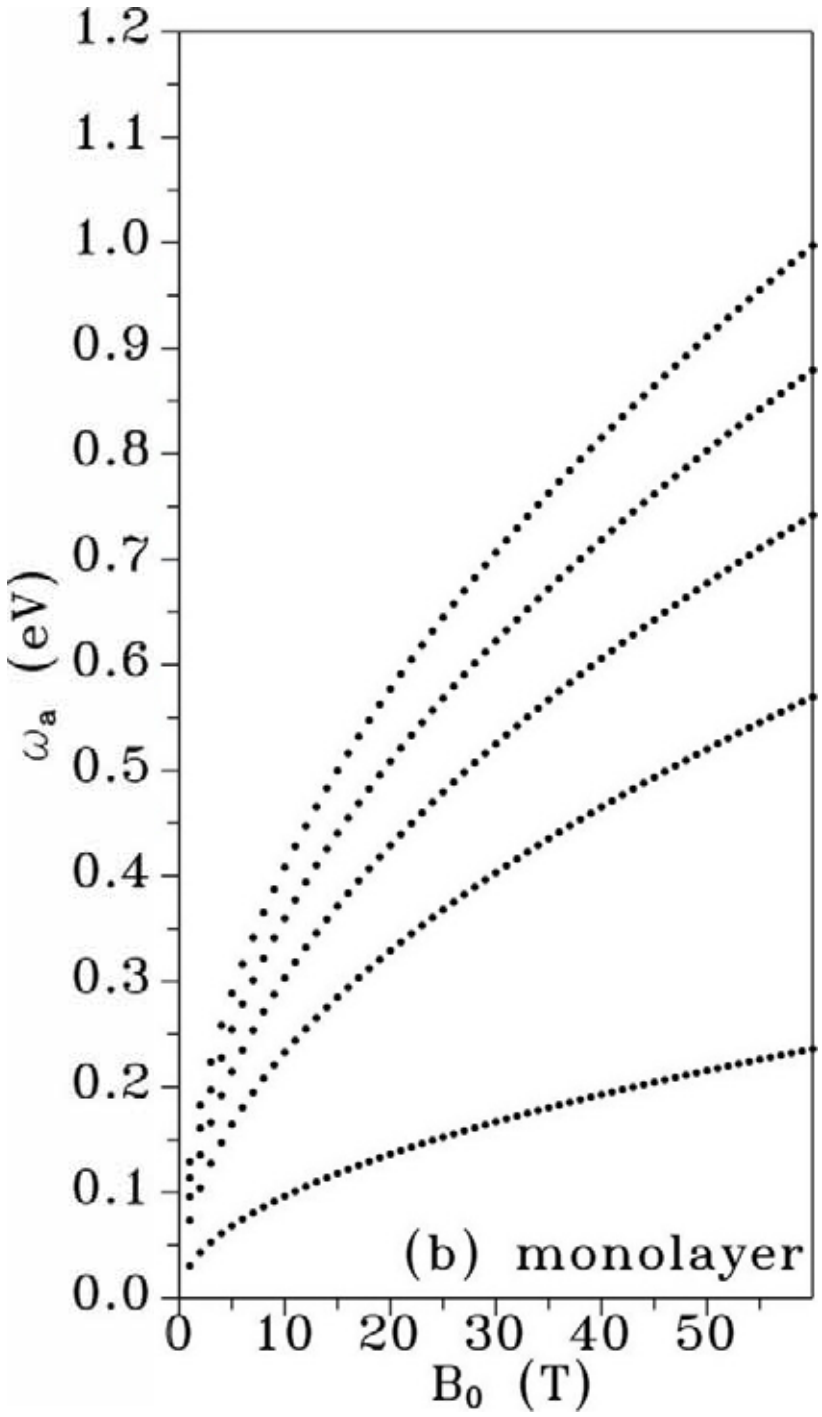

B-dependent absorption frequencies

$2\gamma_1 = 0.73$ eV

$\gamma_1 - \gamma_6 = 0.39$ eV

$\gamma_1 + \gamma_6 = 0.34$ eV

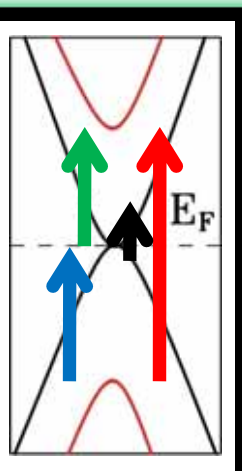

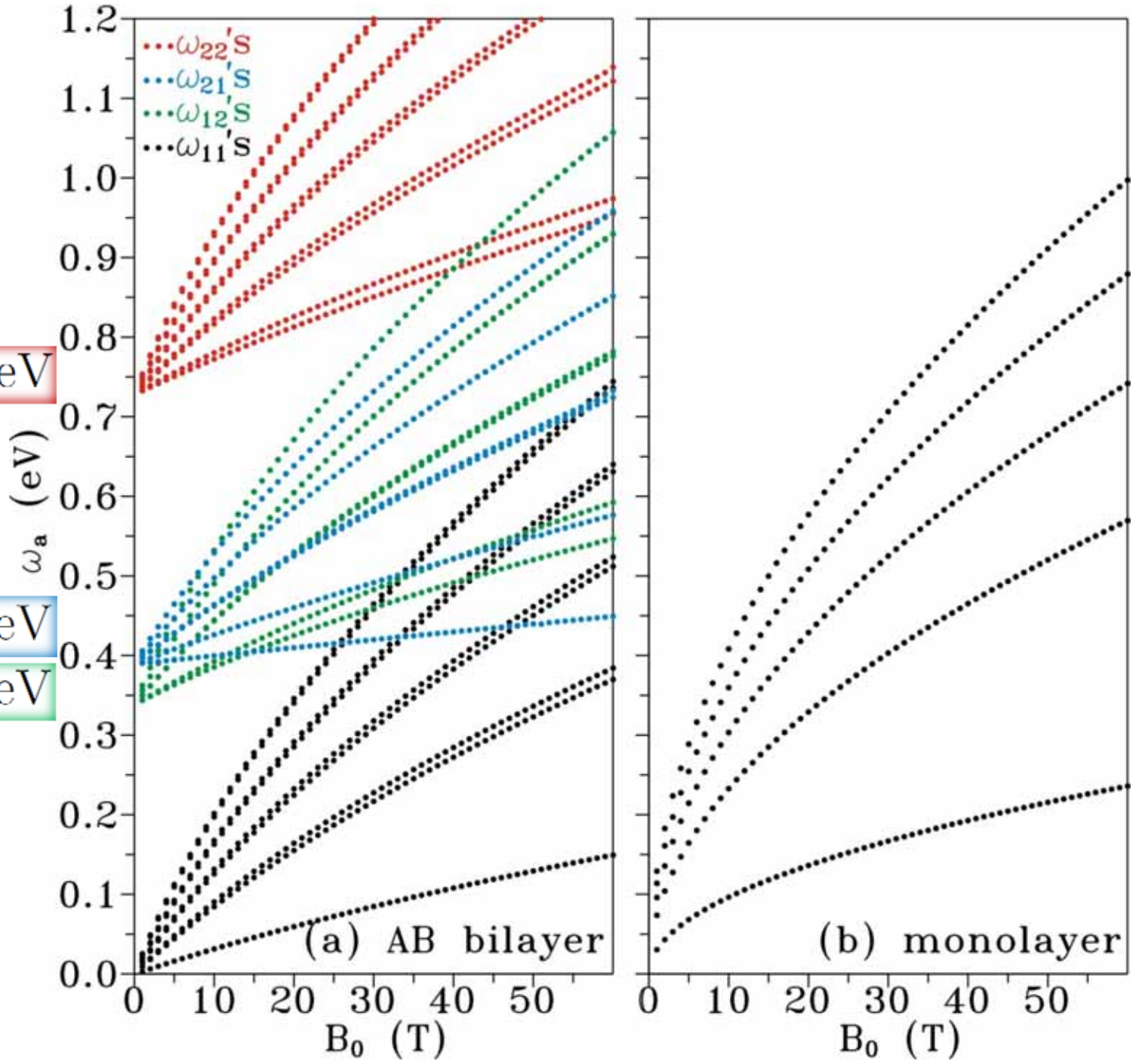

Summary…

Interlayer interactions alter Landau energies and Landau wave functions, break the symmetry of valence and conduction states, and most importantly, bring about the second group of Landau levels.

Optical excitations between the two groups of Landau levels lead to four kinds of absorption peaks.

Thanks for your attention !

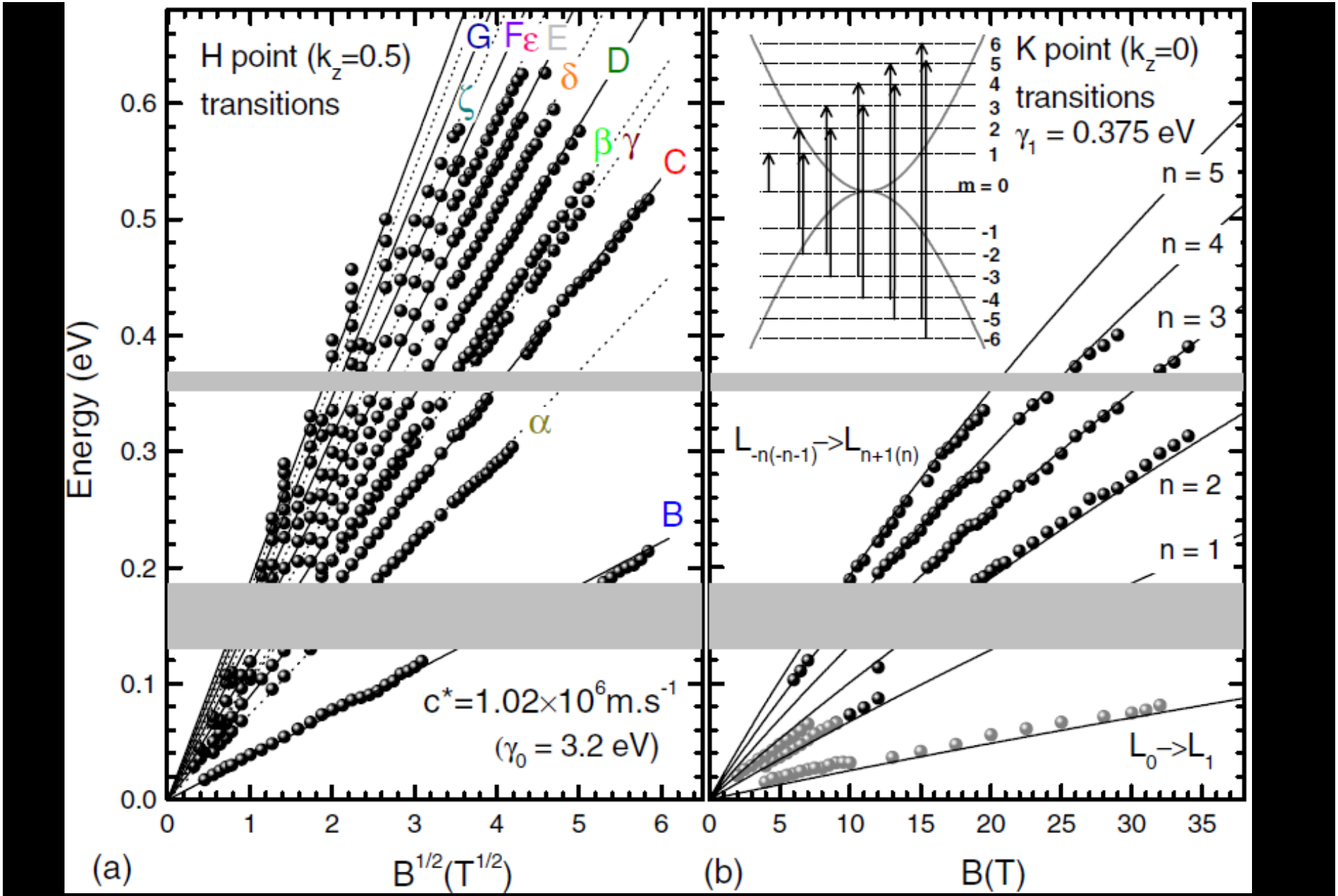

M. Orlita, C. Faugeras, J. M. Schneider, G. Martinez, D. K. Maude, and M. Potemski,
PRL 102, 166401 (2009)

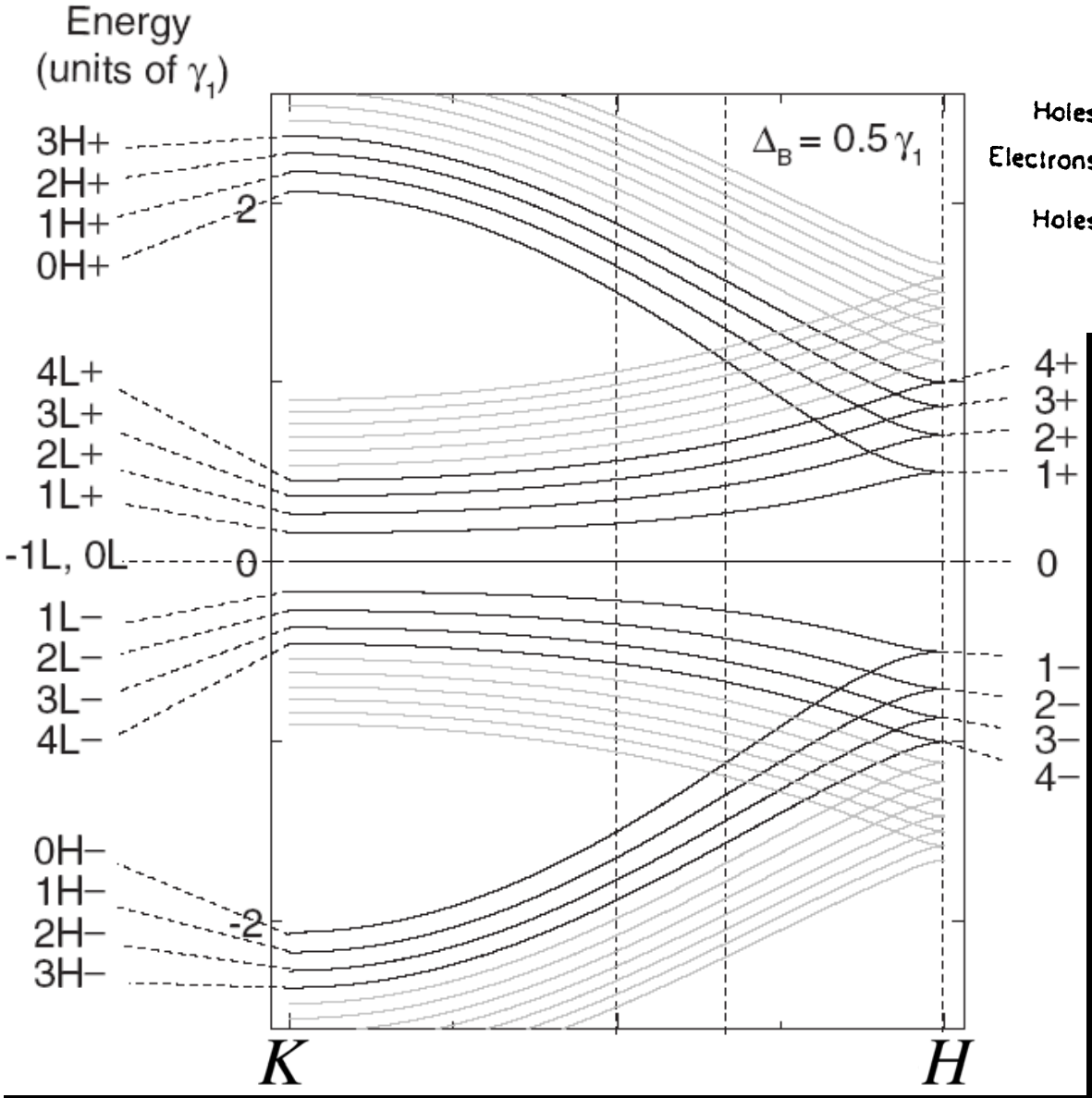

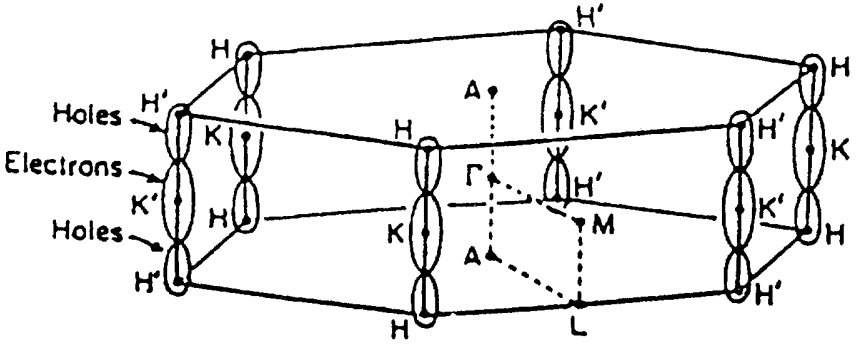

M. Koshino, T. Ando, **PRB 77, 115313 (2008)**

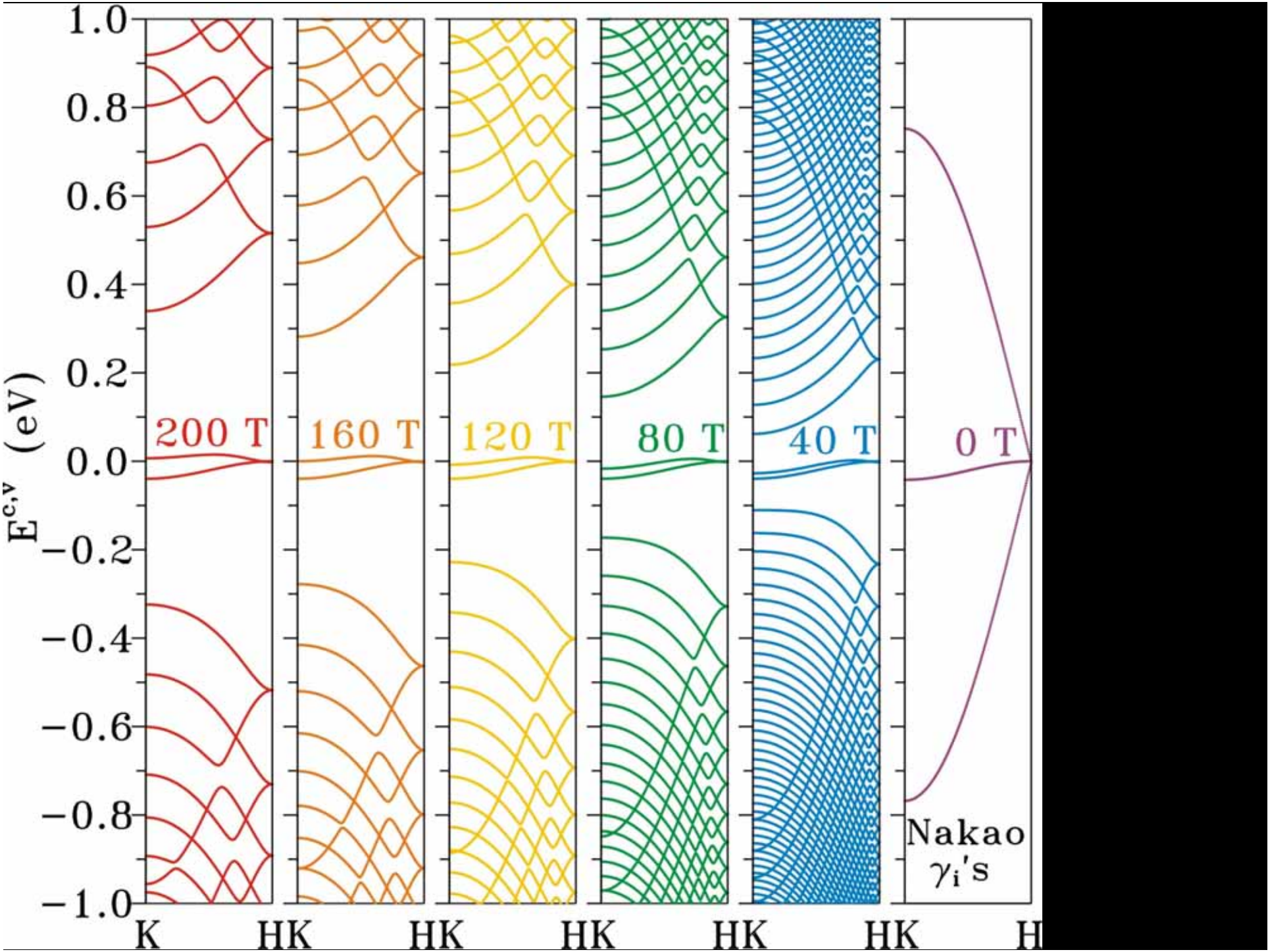
1.0
0.8
0.6
0.4
0.2
0.0
−0.2
−0.4
−0.6
−0.8
−1.0
E^{c,v} (eV)
200 T
160 T
120 T
80 T
40 T
0 T
Nakao
γi's
K
HK
HK
HK
HK
HK
H

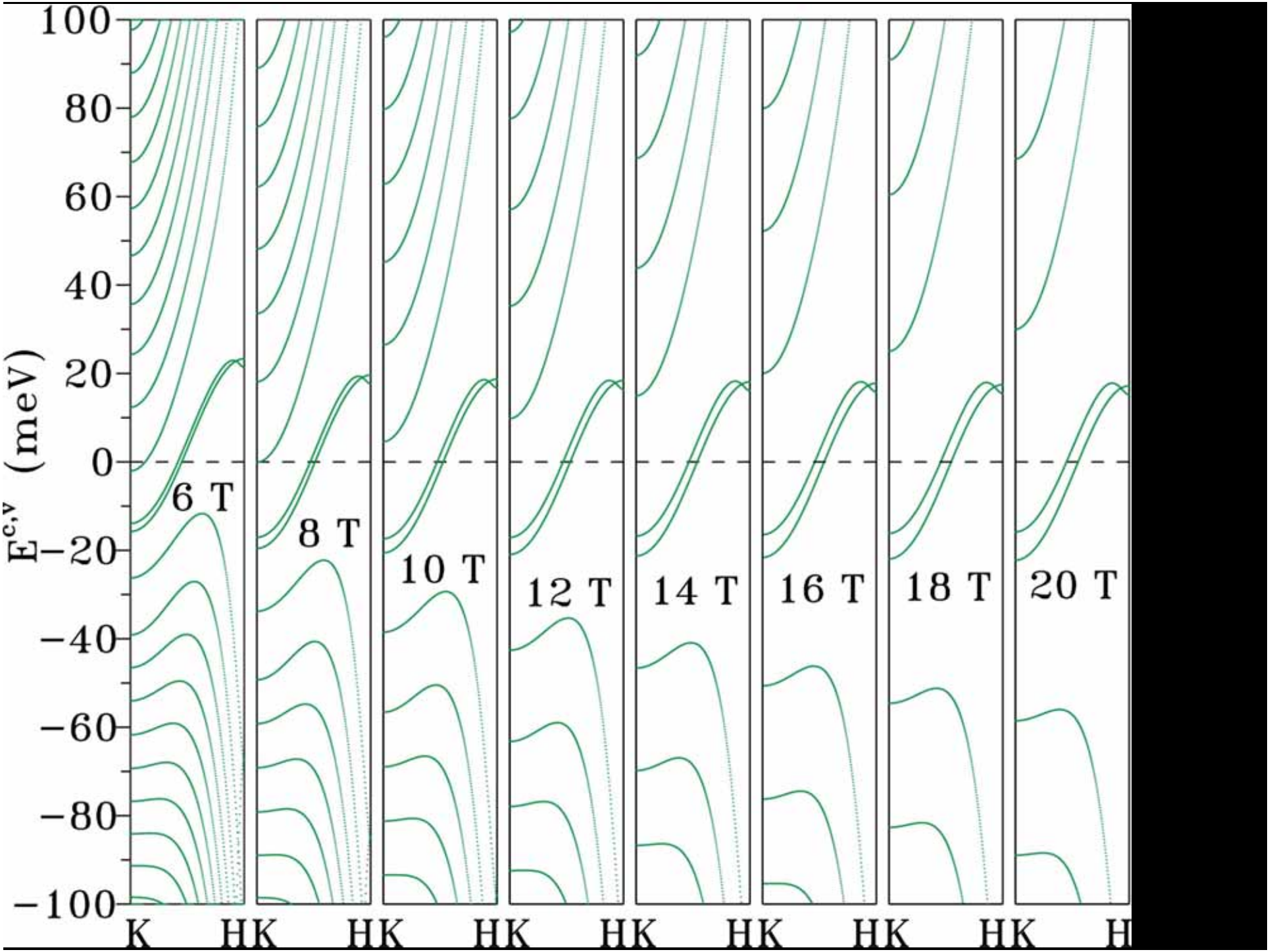
100
80
60
40
20
0
−20
−40
−60
−80
−100
E^{c,v} (meV)
6 T
8 T
10 T
12 T
14 T
16 T
18 T
20 T
K
HK
HK
HK
HK
HK
HK
HK
H

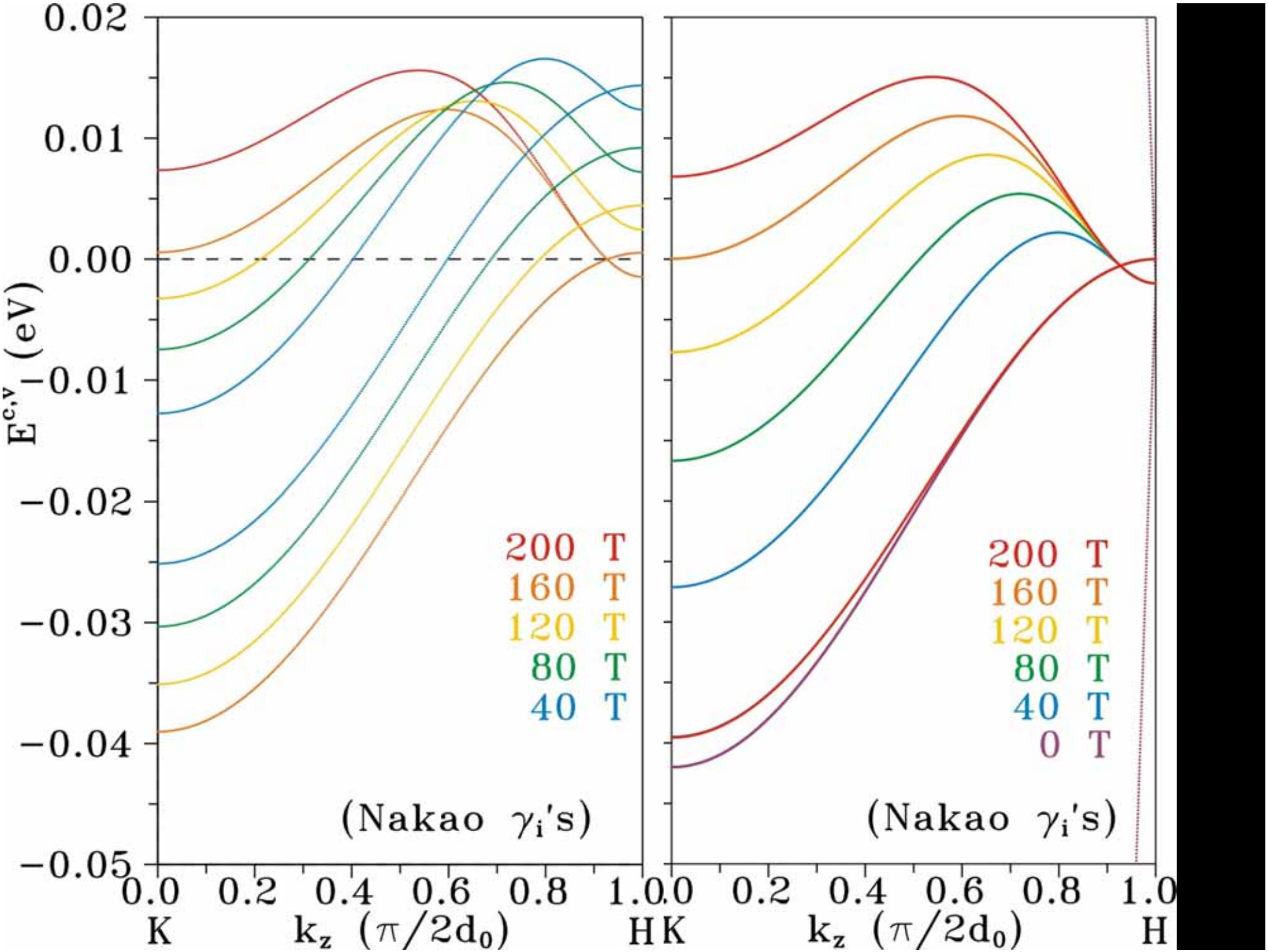
0.02
0.01
0.00
−0.01
−0.02
−0.03
−0.04
−0.05
$E^{c,v}_l$ (eV)
200 T
160 T
120 T
80 T
40 T
(Nakao γ_i's)
0.0 0.2 0.4 0.6 0.8 1.0
K
k_z ($\pi/2d_0$)
H
200 T
160 T
120 T
80 T
40 T
0 T
(Nakao γ_i's)
0.0 0.2 0.4 0.6 0.8 1.0
K
k_z ($\pi/2d_0$)
H

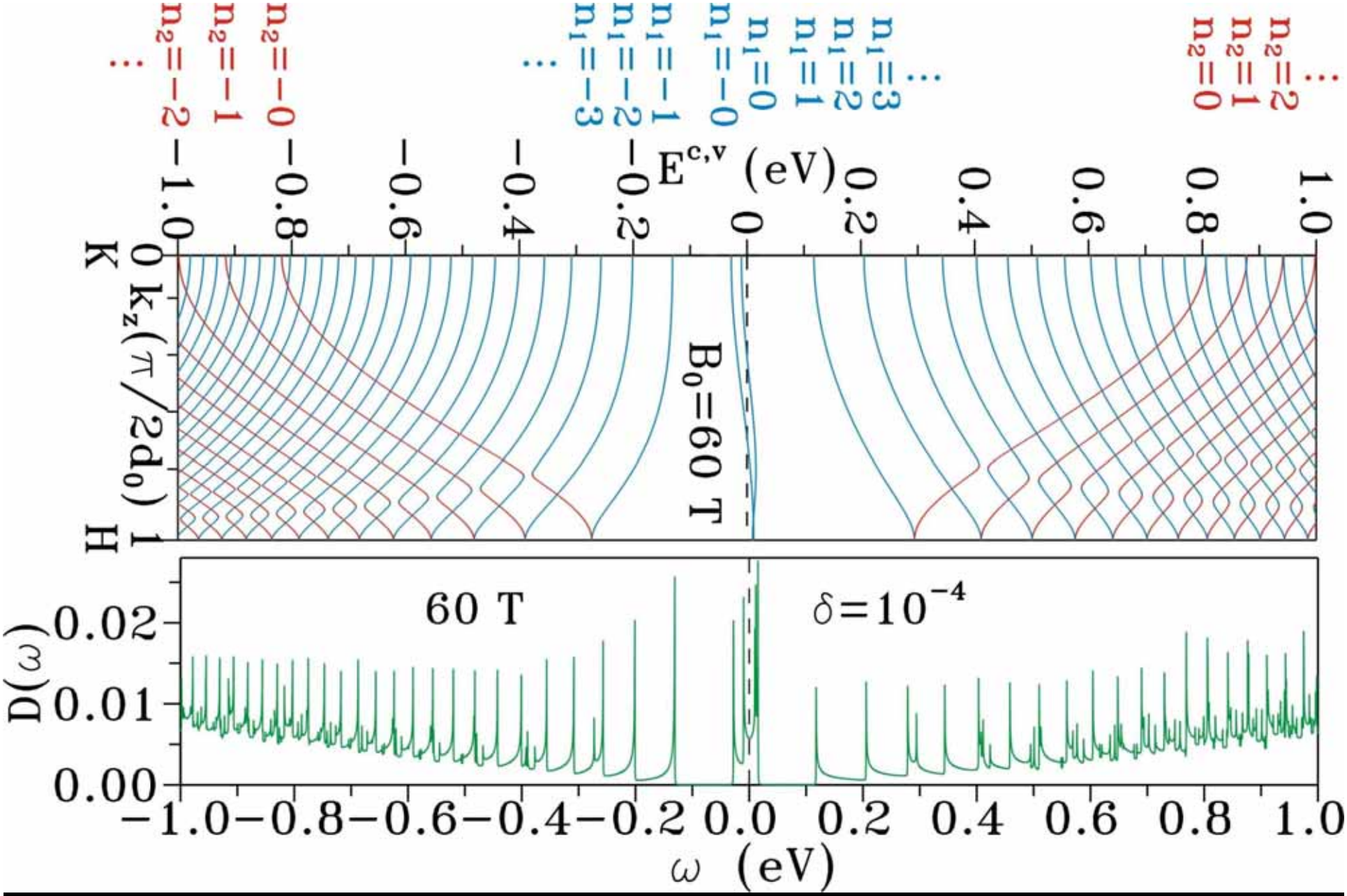

Intensity: $K > H > K\bar{H}$

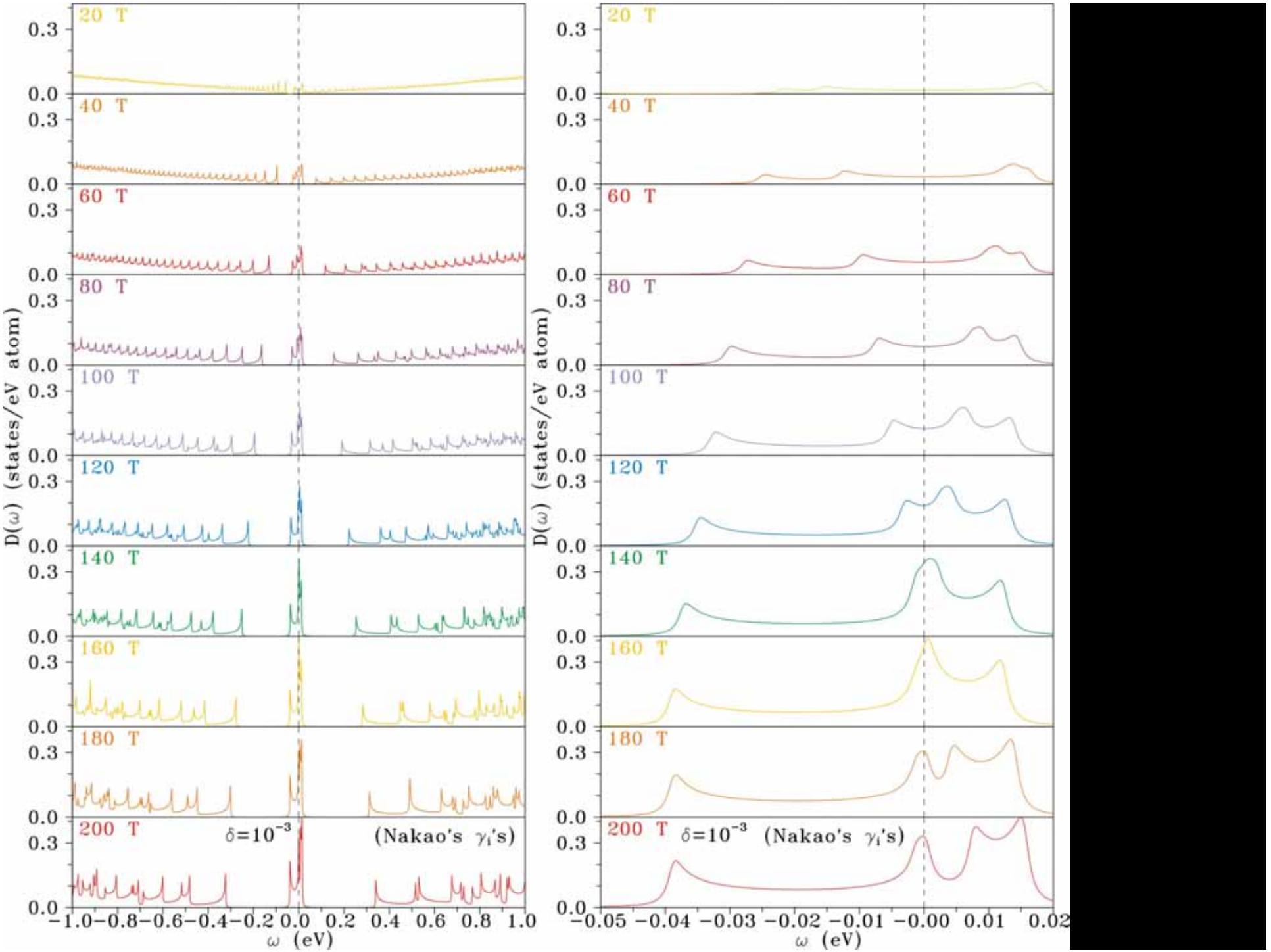
20 T
40 T
60 T
80 T
100 T
120 T
140 T
160 T
180 T
200 T
δ=10⁻³
(Nakao's γᵢ's)
D(ω) (states/eV atom)
ω (eV)
0.0
0.3
−1.0 −0.8 −0.6 −0.4 −0.2 0.0 0.2 0.4 0.6 0.8 1.0
−0.05 −0.04 −0.03 −0.02 −0.01 −0.00 0.01 0.02

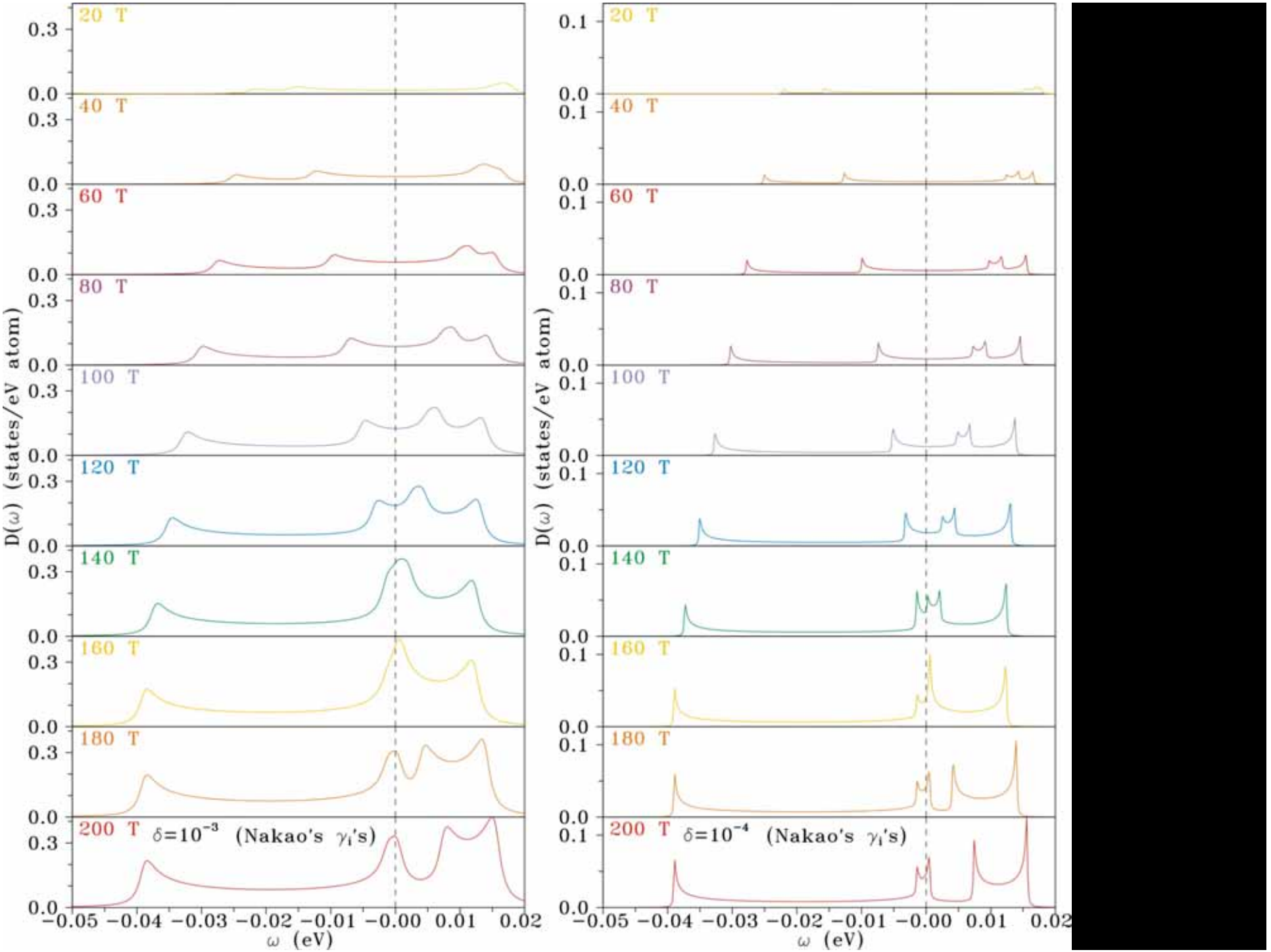
20 T
40 T
60 T
80 T
100 T
120 T
140 T
160 T
180 T
200 T
δ=10^-3 (Nakao's γi's)
δ=10^-4 (Nakao's γi's)
D(ω) (states/eV atom)
ω (eV)
0.3
0.0
0.1
−0.05 −0.04 −0.03 −0.02 −0.01 −0.00 0.01 0.02

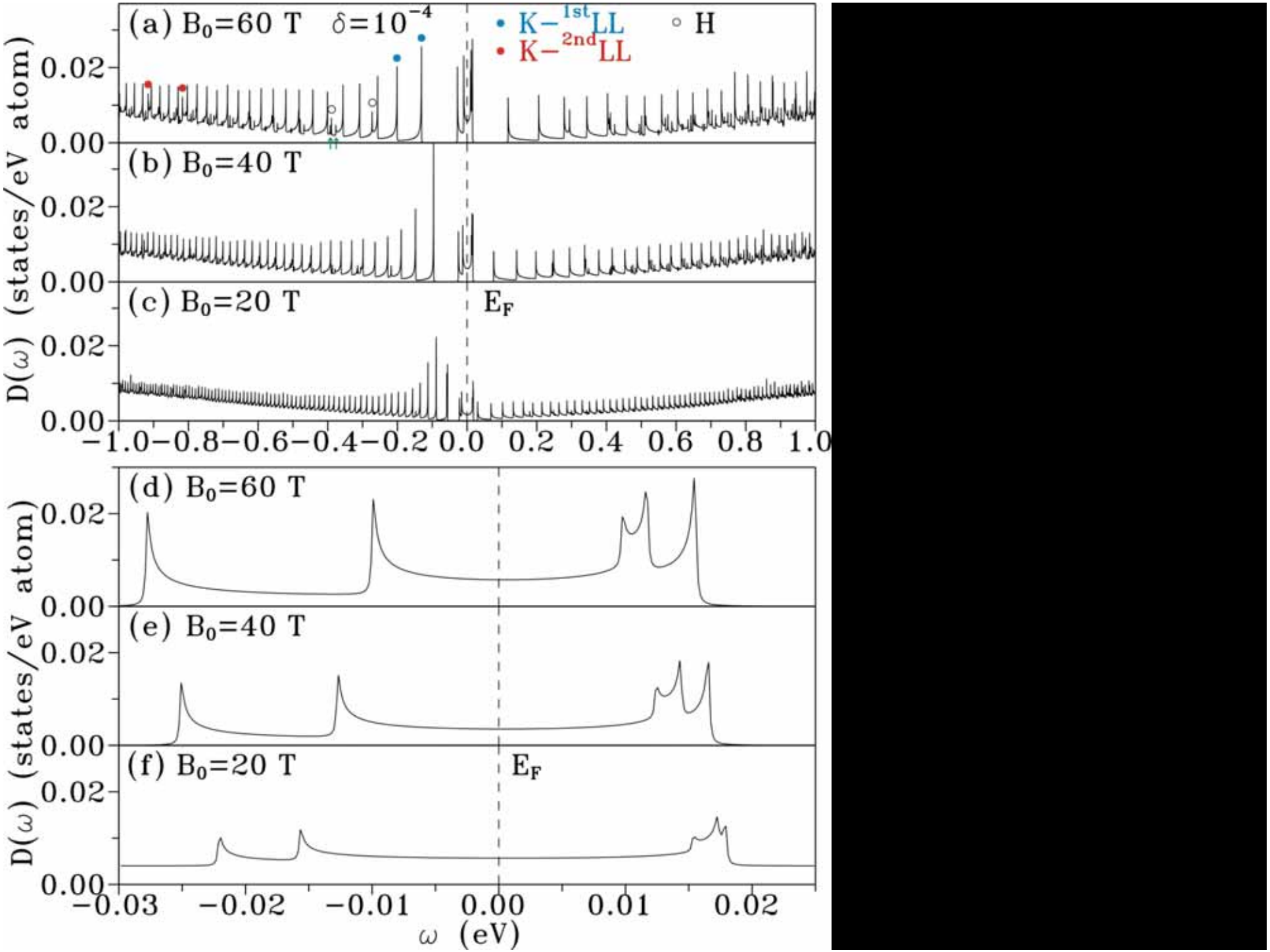
(a) B0=60 T δ=10−4
K−1st LL
K−2nd LL
H
(b) B0=40 T
(c) B0=20 T
EF
D(ω) (states/eV atom)
0.02
0.00
−1.0 −0.8 −0.6 −0.4 −0.2 0.0 0.2 0.4 0.6 0.8 1.0
(d) B0=60 T
(e) B0=40 T
(f) B0=20 T
EF
−0.03 −0.02 −0.01 0.00 0.01 0.02
ω (eV)

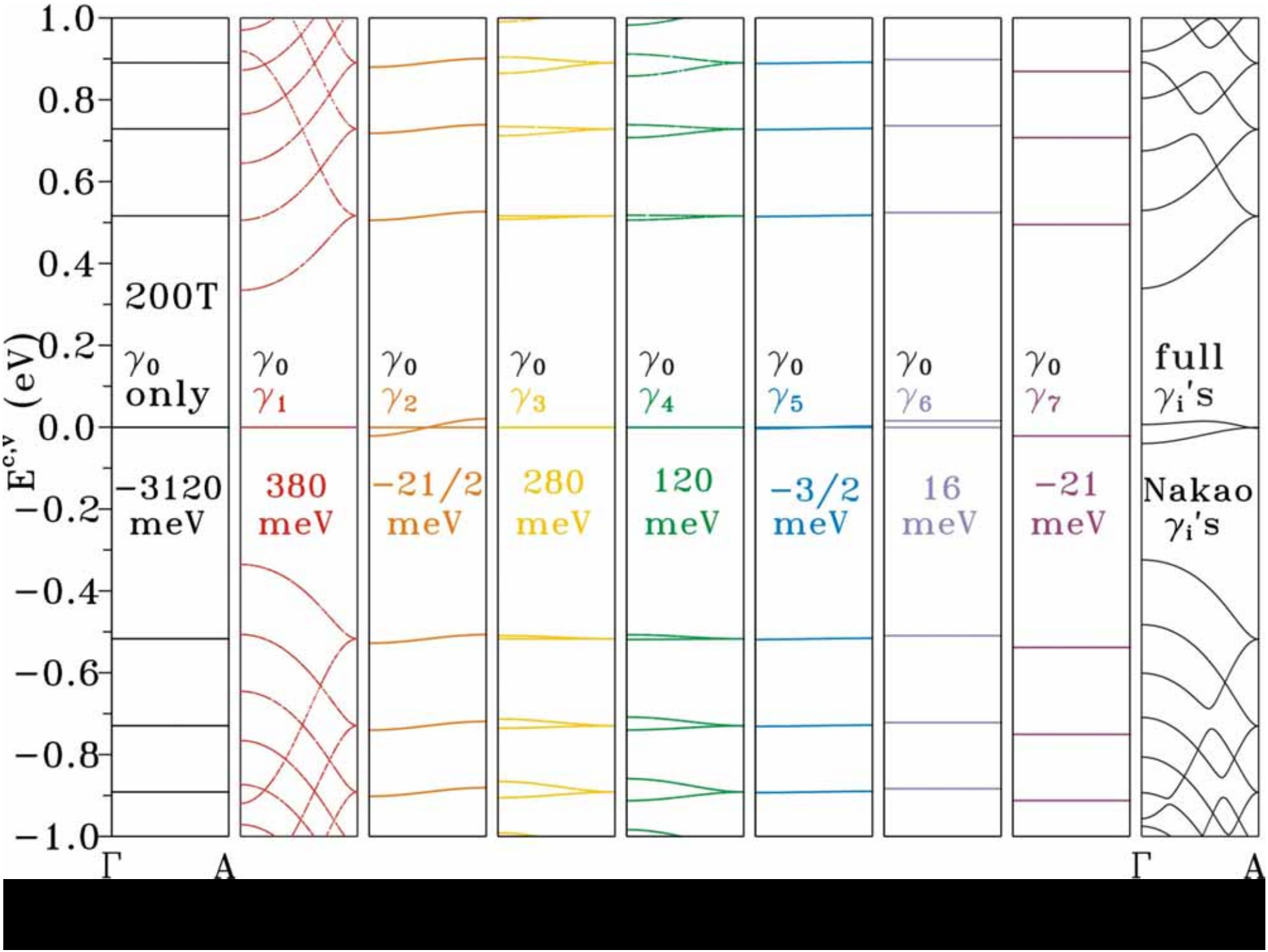
1.0
0.8
0.6
0.4
0.2
0.0
−0.2
−0.4
−0.6
−0.8
−1.0
E^{c,v} (eV)
200T
γ0
only
−3120
meV
γ0
γ1
380
meV
γ0
γ2
−21/2
meV
γ0
γ3
280
meV
γ0
γ4
120
meV
γ0
γ5
−3/2
meV
γ0
γ6
16
meV
γ0
γ7
−21
meV
full
γi's
Nakao
γi's
Γ
A
Γ
A

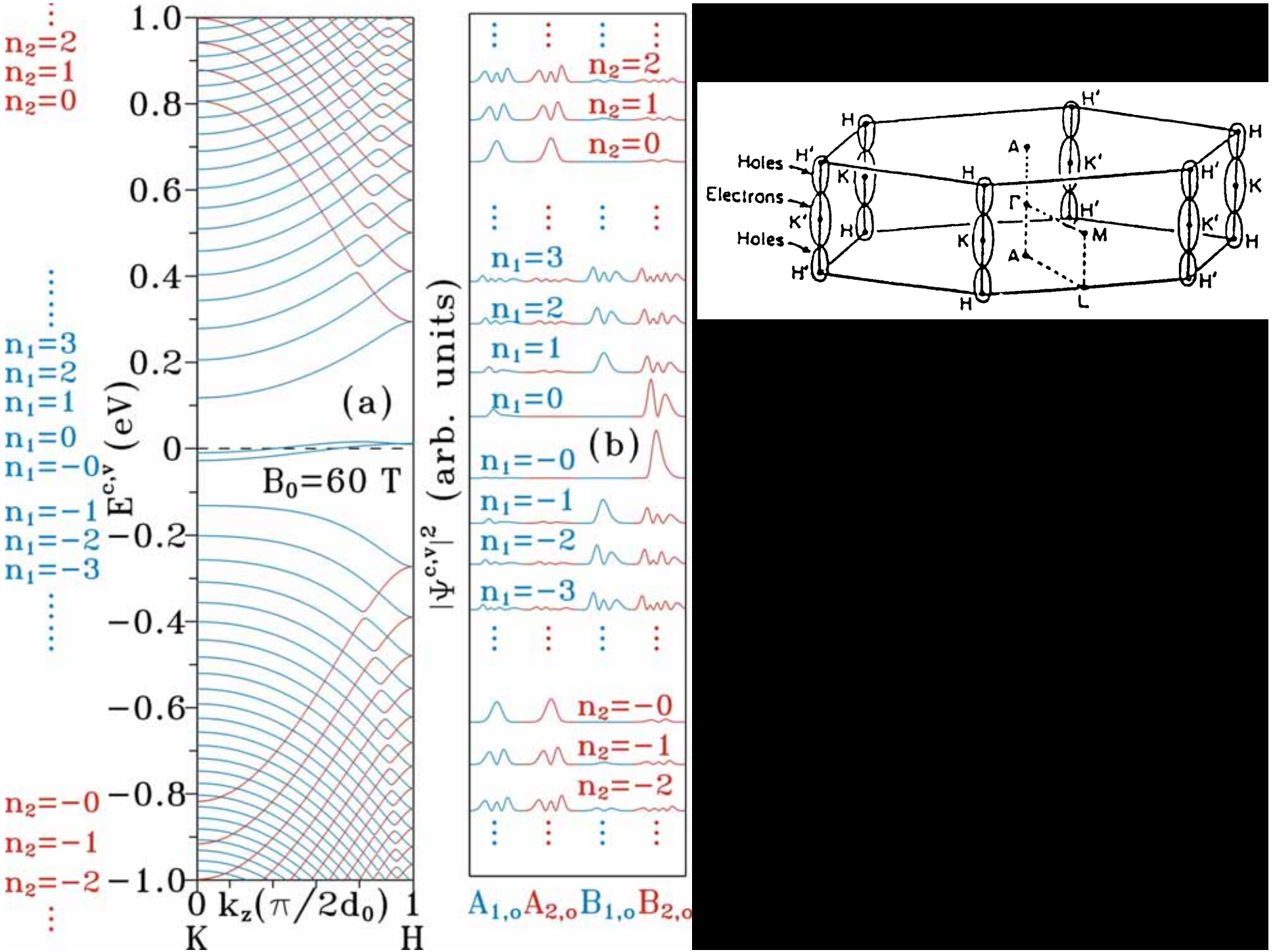
n2=2
n2=1
n2=0
n1=3
n1=2
n1=1
n1=0
n1=−0
n1=−1
n1=−2
n1=−3
n2=−0
n2=−1
n2=−2
1.0
0.8
0.6
0.4
0.2
0
−0.2
−0.4
−0.6
−0.8
−1.0
E^{c,v} (eV)
(a)
B0=60 T
0 kz(π/2d0) 1
K
H
|Ψ^{c,v}|^2 (arb. units)
n2=2
n2=1
n2=0
n1=3
n1=2
n1=1
n1=0
n1=−0
n1=−1
n1=−2
n1=−3
n2=−0
n2=−1
n2=−2
(b)
A1,o A2,o B1,o B2,o
H'
H
A
K'
K
Γ
M
L
Holes
Electrons
Holes

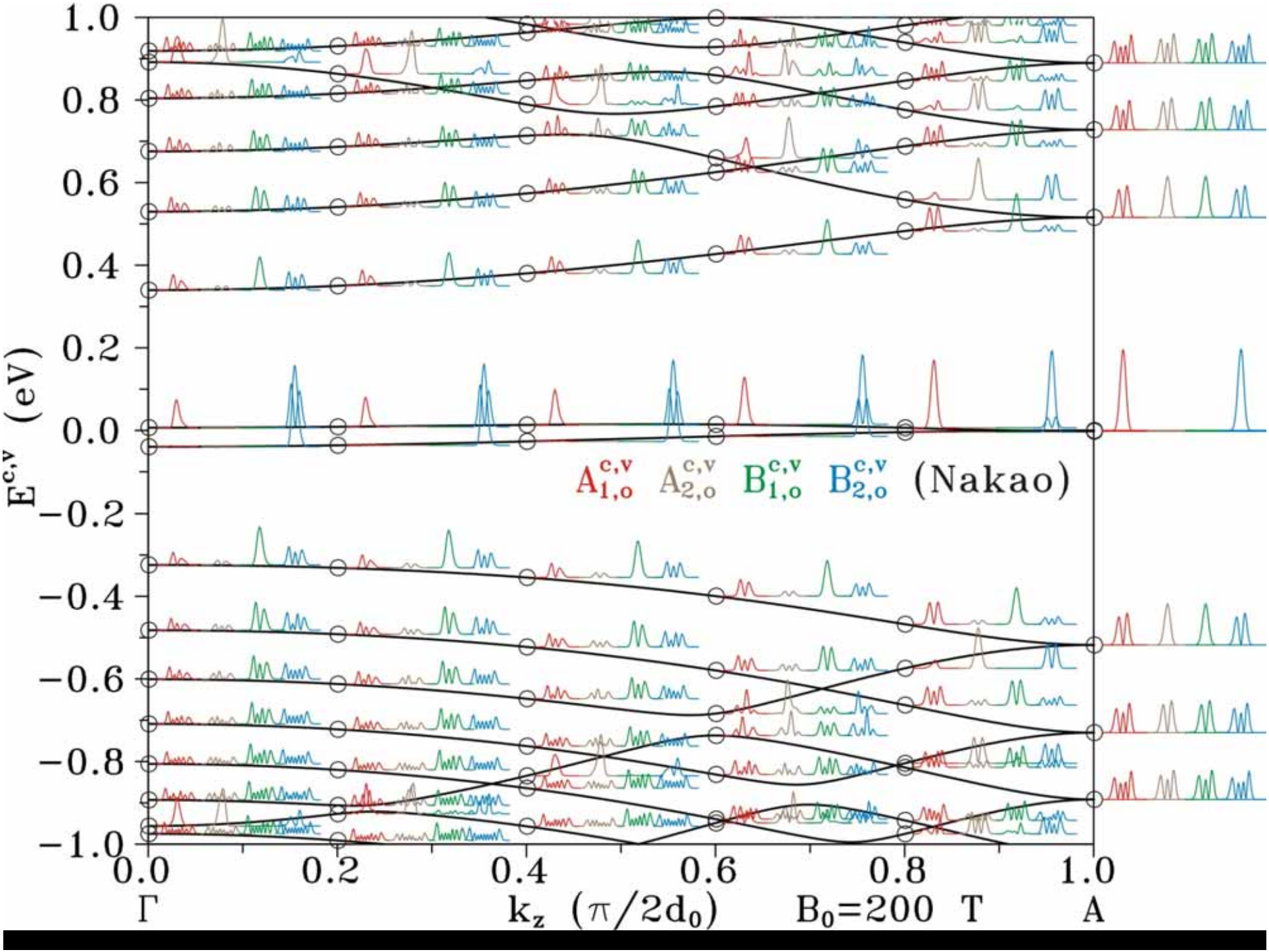
1.0
0.8
0.6
0.4
0.2
0.0
−0.2
−0.4
−0.6
−0.8
−1.0
E^{c,v} (eV)
A^{c,v}_{1,o} A^{c,v}_{2,o} B^{c,v}_{1,o} B^{c,v}_{2,o} (Nakao)
0.0
0.2
0.4
0.6
0.8
1.0
Γ
k_z (π/2d_0)
B_0=200 T
A

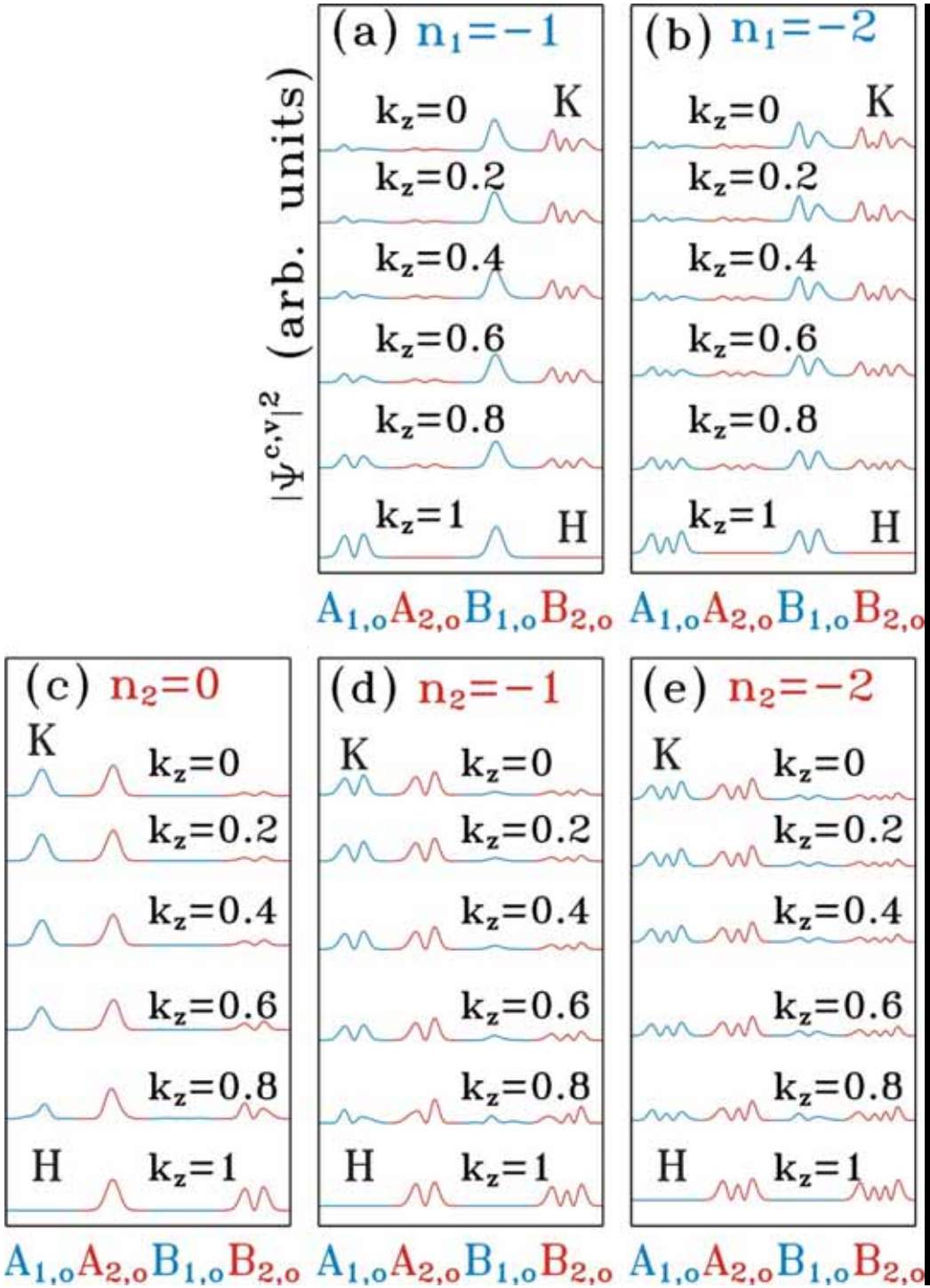
(a) $n_1=-1$
(b) $n_1=-2$
(c) $n_2=0$
(d) $n_2=-1$
(e) $n_2=-2$
$|\Psi^{c,v}|^2$ (arb. units)
$k_z=0$
$k_z=0.2$
$k_z=0.4$
$k_z=0.6$
$k_z=0.8$
$k_z=1$
K
H
$A_{1,o}A_{2,o}B_{1,o}B_{2,o}$

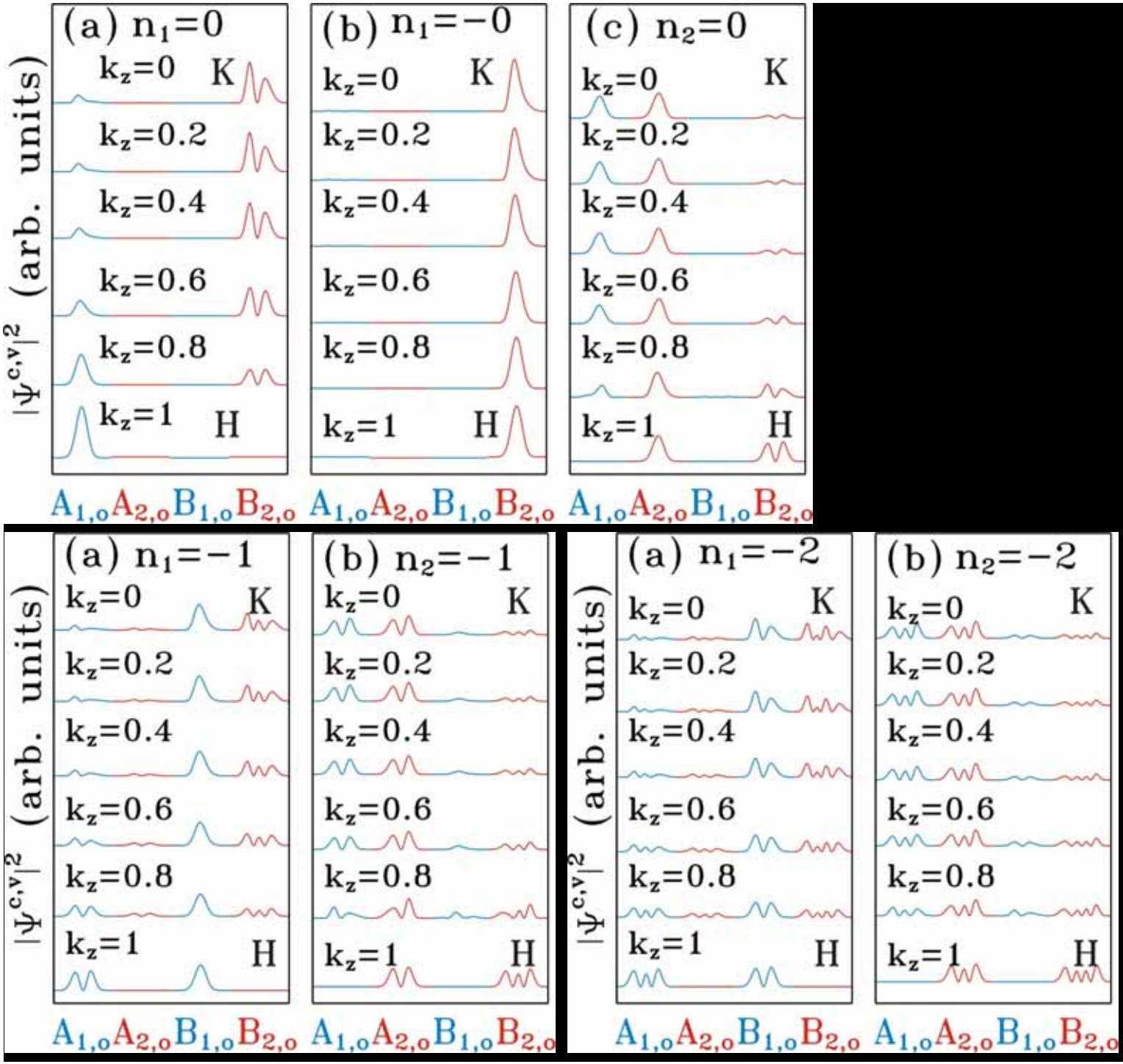
(a) $n_1=0$
(b) $n_1=-0$
(c) $n_2=0$
(a) $n_1=-1$
(b) $n_2=-1$
(a) $n_1=-2$
(b) $n_2=-2$
$|\Psi^{c,v}|^2$ (arb. units)
$k_z=0$ K
$k_z=0.2$
$k_z=0.4$
$k_z=0.6$
$k_z=0.8$
$k_z=1$ H
$A_{1,o}A_{2,o}B_{1,o}B_{2,o}$

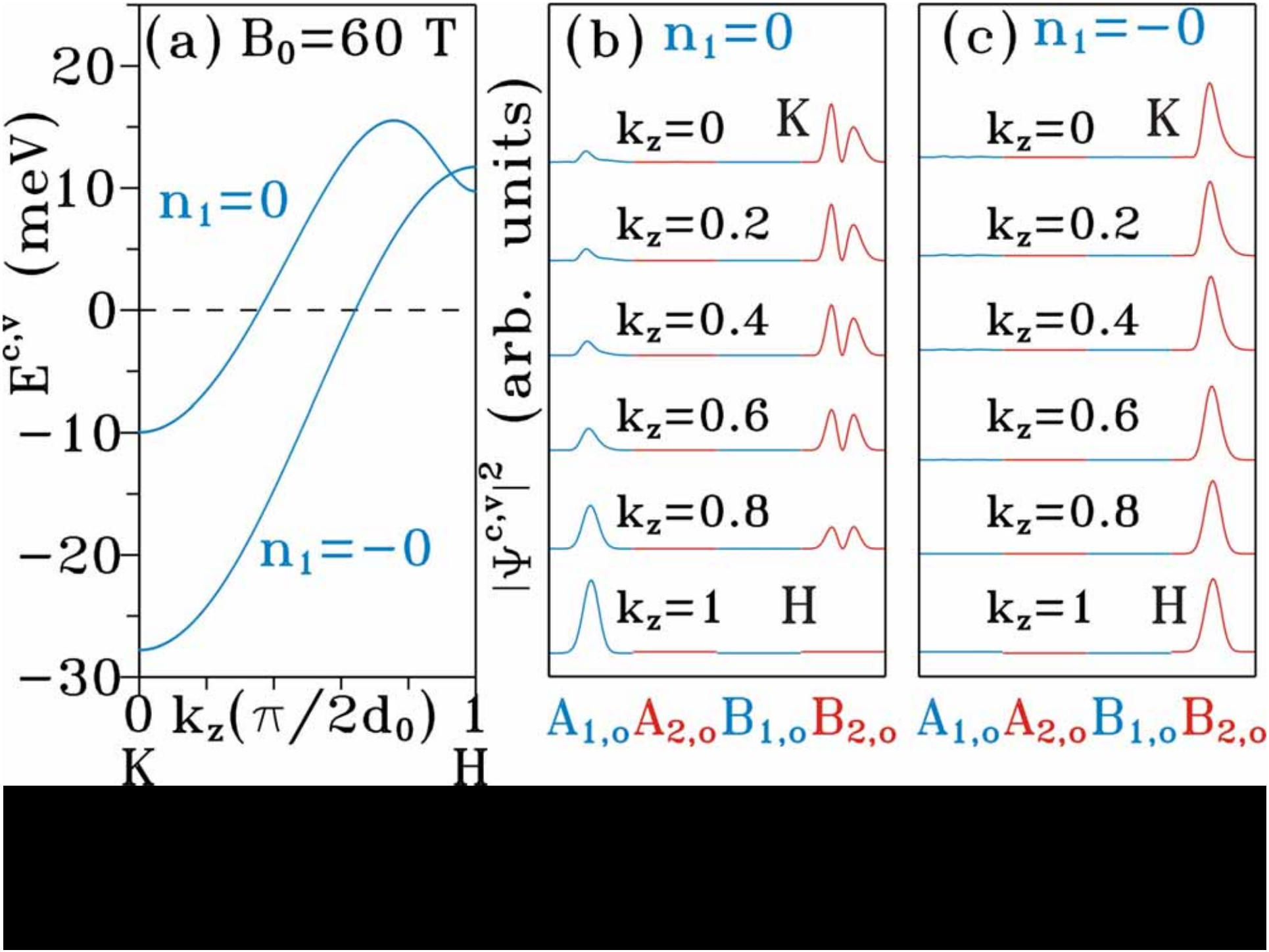
(a) B_0=60 T
20
10
0
−10
−20
−30
$E^{c,v}$ (meV)
n_1=0
n_1=−0
0 $k_z(\pi/2d_0)$ 1
K
H
(b) n_1=0
(c) n_1=−0
$|\Psi^{c,v}|^2$ (arb. units)
k_z=0 K
k_z=0.2
k_z=0.4
k_z=0.6
k_z=0.8
k_z=1 H
$A_{1,o}A_{2,o}B_{1,o}B_{2,o}$
$A_{1,o}A_{2,o}B_{1,o}B_{2,o}$

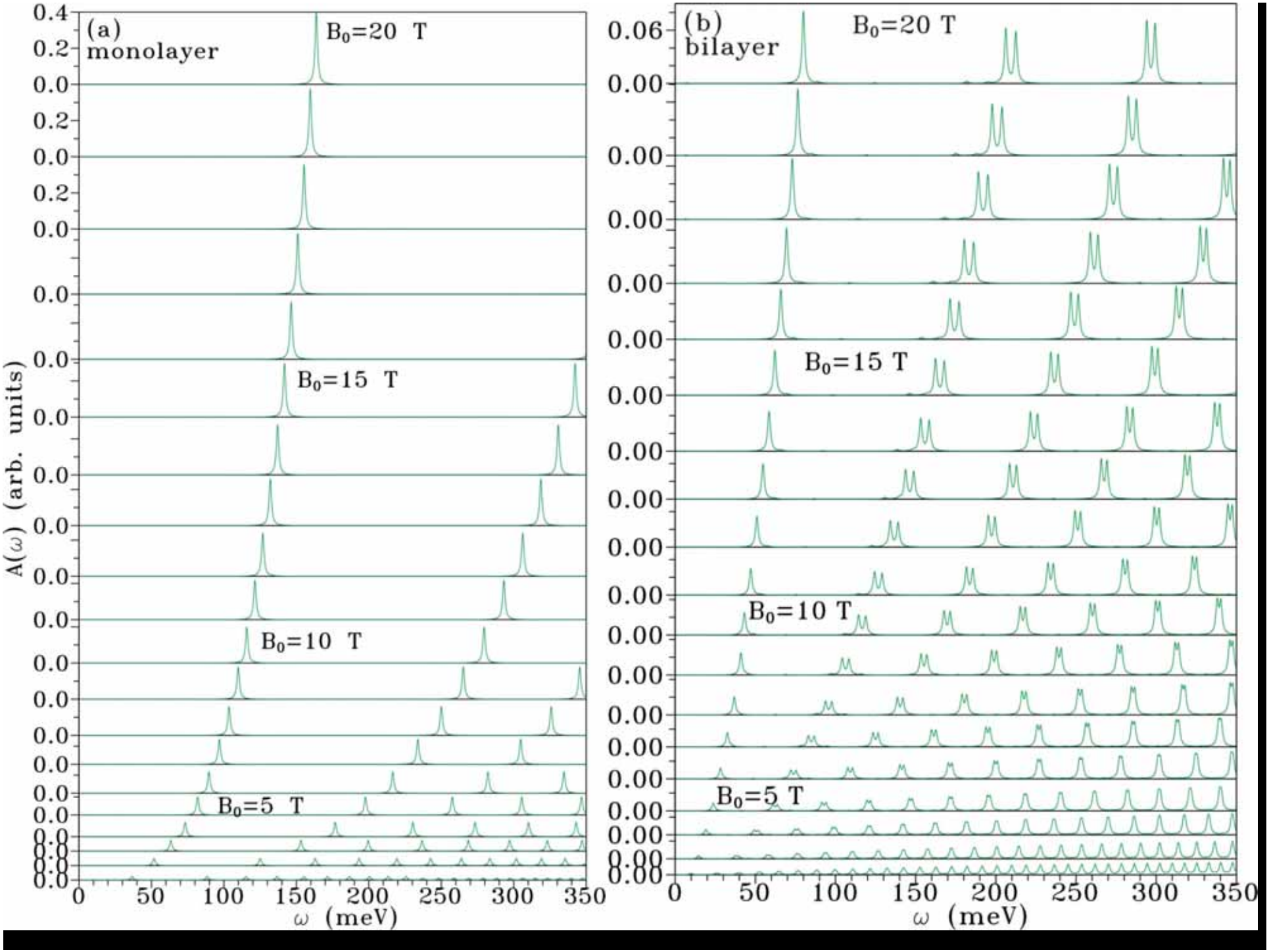
(a)
monolayer
B0=20 T
B0=15 T
B0=10 T
B0=5 T
A(ω) (arb. units)
ω (meV)
(b)
bilayer
B0=20 T
B0=15 T
B0=10 T
B0=5 T
ω (meV)